FIG. 1. Human IECs constitutively produce IL-7, and IL-1, TNF-α, and TGF-β do not influence the levels of IL-7 production, whereas IFN-γ does. DLD-1 and HT29-18N2 cells were cultured in medium alone or in medium containing 50 ng of either IL-1, TNF-α, TGF-β, IFN-γ, or IFN-γ plus TGF-β per ml for 24 h. The supernatants were collected and assayed for IL-7 production by ELISA. Results are the means ± standard deviations of three independent experiments. *, $P <$ 0.05 by a paired Student $t$ test.

**induces short species of mRNA via a selective usage of downstream initiation sites.** Human tissues have been shown to express two major IL-7 mRNAs of ~1.8 and ~2.4 kb, and this has been inferred as a result of alternative polyadenylation (8). To examine whether constitutive and IFN-γ-inducible IL-7 protein production is regulated at the mRNA level, we next assessed the expression of IL-7 transcripts by Northern blot analysis by using a cDNA probe covering the IL-7 protein coding sequences (Fig. 2A, CS probe). In DLD-1 cells, two major mRNA species were clearly observed in the absence of IFN-γ (Fig. 2B, left). Since each of these bands migrated somewhat heterogeneously, it was difficult to determine the precise size of these transcripts. However, the analysis of mRNAs extracted from SK-Hep1 cells, human hepatocellular carcinoma cells originally used for the cloning of the human IL-7 gene (8), showed equally migrating bands (data not shown). Thus, we tentatively equated these transcripts with those described previously (8). When DLD-1 cells were treated with IFN-γ, ~1.8-kb mRNA was significantly induced within 6 h, whereas the increase in ~2.4-kb mRNA was modest (Fig. 2B, left). Although the basal level of IL-7 mRNA was lower in HT29-18N2 cells than could be visualized, these cells displayed a similar pattern of IL-7 mRNA expression: IFN-γ significantly induced expression of ~1.8-kb and, to a lesser extent, ~2.4-kb of mRNAs (Fig. 2B, right). These data indicated that the levels of IL-7 protein production correlate well with those of mRNA expression and that IFN-γ treatment predominantly induces the short mRNA species of the IL-7 gene. Interestingly, in murine keratinocytes, IFN-γ treatment was demonstrated to induce the expression of relatively short species of IL-7 mRNA through the use of alternative transcription start sites (3). Given an analogy in IFN-γ-dependent induction of selective IL-7 transcripts between human IECs and murine keratinocytes, it seemed possible that the mechanisms of IFN-γ-depen-

dent IL-7 gene expression are, at least in part, conserved between these two cell types.

To date, a detailed analysis of the transcription start sites for the human IL-7 gene has not been reported. We thus at-
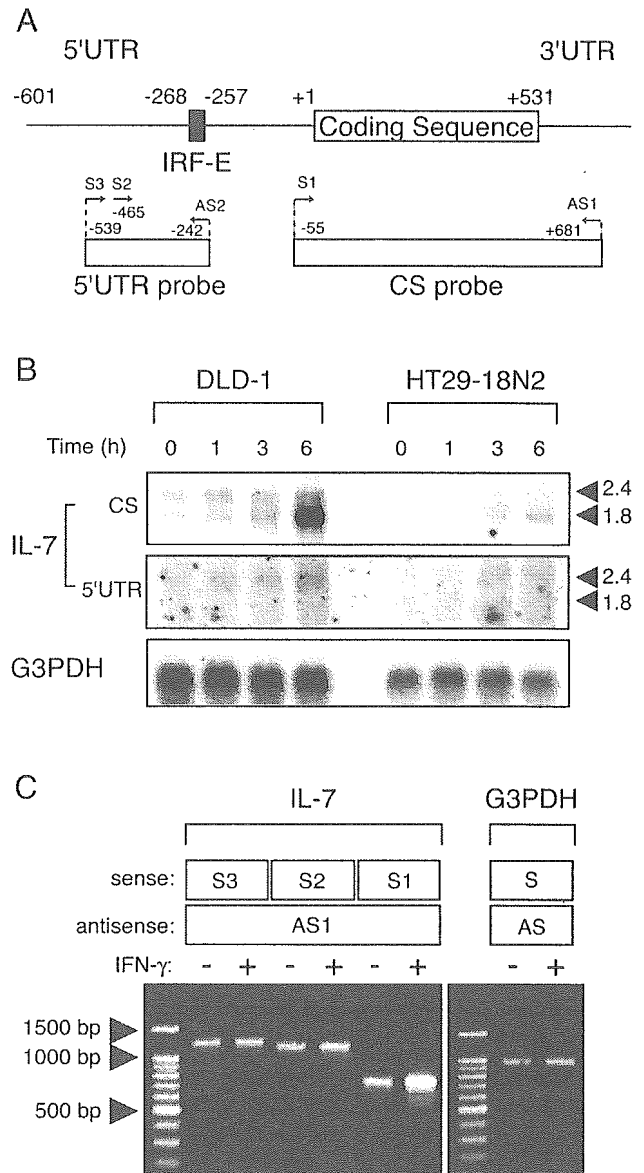






FIG. 2. IFN-γ-dependent and -independent IL-7 production is distinctively regulated by expression of IL-7 transcripts that differ in their 5′ UTR. (A) Schematic drawing of human IL-7 mRNA, with the primers and cDNA probes used in this study. The nucleotide number was designated with respect to the translation start site (+1). An IRF-E located at the region from position −268 to −257 is also indicated. (B) DLD-1 and HT29-18N2 cells were stimulated with IFN-γ (50 ng/ml) for the indicated time periods. Fifteen micrograms of poly(A)+ mRNA was subjected to Northern blotting for IL-7 mRNA by using the 32P-labeled CS probe or the 5′ UTR probe. The bottom panel indicates the level of G3PDH mRNA as a control. (C) DLD-1 cells were treated with IFN-γ (50 ng/ml) or left untreated for 6 h, collected for total RNA isolation, and then subjected to semiquantitative RT-PCR for IL-7 mRNA. PCR amplification was performed by using either the S1, S2, or S3 primer along with AS1 primer depicted in panel A. As controls, samples from IFN-γ-treated and untreated cells were amplified with a primer set for G3PDH.

A

B

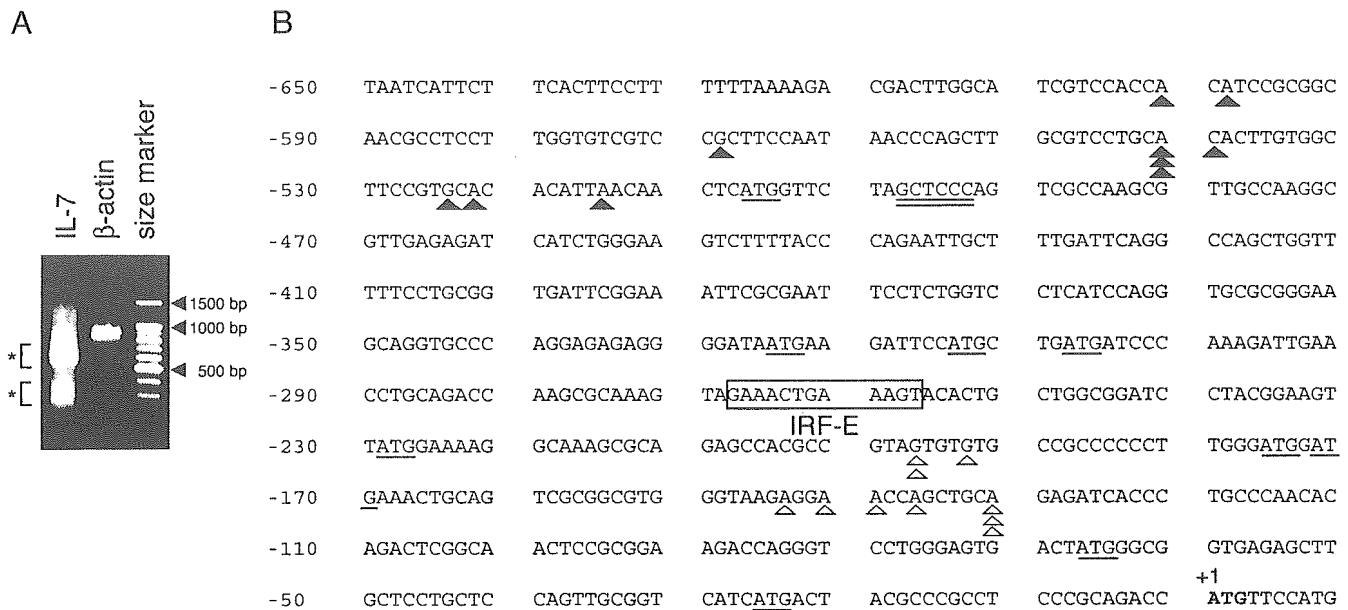| | | | | | | |
|---|---|---|---|---|---|---|
| -650 | TAATCATTCT | TCACTTCCTT | TTTTAAAAGA | CGACTTGGCA | TCGTCCACCA | CATCCGCGGC |
| -590 | AACGCCTCCT | TGGTGTCGTC | CGCTTCCAAT | AACCCAGCTT | GCGTCCTGCA | CACTTGTGGC |
| -530 | TTCCGTGCAC | ACATTAACAA | CTCATGGTTC | TAGCTCCCAG | TCGCCAAGCG | TTGCCAAGGC |
| -470 | GTTGAGAGAT | CATCTGGGAA | GTCTTTTACC | CAGAATTGCT | TTGATTCAGG | CCAGCTGGTT |
| -410 | TTTCCTGCGG | TGATTCGGAA | ATTCGCGAAT | TCCTCTGGTC | CTCATCCAGG | TGCGCGGGAA |
| -350 | GCAGGTGCCC | AGGAGAGAGG | GGATAATGAA | GATTCCATGC | TGATGATCCC | AAAGATTGAA |
| -290 | CCTGCAGACC | AAGCGCAAAG | TAGAAACTGA     AAGTACACTG | | CTGGCGGATC | CTACGGAAGT |
| | | | IRF-E | | | |
| -230 | TATGGAAAAG | GCAAAGCGCA | GAGCCACGCC | GTAGTGTGTG | CCGCCCCCCT | TGGGATGGAT |
| -170 | GAAACTGCAG | TCGCGGCGTG | GGTAAGAGGA | ACCAGCTGCA | GAGATCACCC | TGCCCAACAC |
| -110 | AGACTCGGCA | ACTCCGCGGA | AGACCAGGGT | CCTGGGAGTG | ACTATGGGCG | GTGAGAGCTT |
| | | | | | | +1 |
| -50 | GCTCCTGCTC | CAGTTGCGGT | CATCATGACT | ACGCCCGCCT | CCCGCAGACC | ATGTTCCATG |

FIG. 3. Transcription initiation sites for the human IL-7 gene were clustered within two separate regions upstream from the translation start site. (A) RLM-RACE analysis was performed by using poly(A)$^+$ RNAs from IFN-γ-treated (6 h) DLD-1 cells as described in Materials and Methods. PCR products amplified by a primer set for the IL-7 or β-actin gene, respectively, were run on 1.5% agarose gel, stained with ethidium bromide, and visualized. (B) Two major fragments of ~600 and ~300 bp shown in panel A were independently cloned, and then 10 clones of each were sequenced. The 5' end of each clone is shown by a filled triangle (clones derived from ~600-bp fragments) or an open triangle (clones from ~300-bp fragments) on the first 650 bp of sequence upstream of the translation start site. The authentic translation start site is indicated in bold. Numbering in base pairs is indicated to the left, with negative numbers representing nucleotides upstream of the ATG. Consensus sequences for the IRF-E are boxed and labeled. Potential translation initiation codons (ATG) are underlined. Consensus sequences for MED-1 are also underlined.

tempted to precisely map the 5' end of IL-7 mRNA by using a RLM-RACE method that ensures the amplification of only full-length transcripts via the elimination of truncated mRNAs (see Materials and Methods). When poly(A)$^+$ RNA extracted from IFN-γ-treated (6 h) DLD-1 cells was analyzed, fragments around 600 and 300 bp were obtained by PCR by using the 5' nested primer and the 3' reverse IL-7 GSP-2 (corresponding to nucleotides 36 to 60 of the IL-7 gene) (Fig. 3A). No product was obtained when RNA was not treated with tobacco acid pyrophosphatases, indicating that these products were derived from full-length mRNA (data not shown). Both of these products appeared to migrate somewhat diffusely when subjected to gel electrophoresis (Fig. 3A). This result was not attributable to experimental artifacts, because PCR amplification with another set of primers, designed for detecting the 5' part of the human β-actin gene, yielded products of the expected size (872 bp) that migrated as a single band from the same sample (Fig. 3A). The ~600- and ~300-bp fragments were independently isolated and cloned, and then 10 clones of each were sequenced. All 20 clones contained the IL-7 gene sequence along with the adapter sequences, showing these clones to be derived from mRNAs retaining complete 5' ends. Alternative splicing appeared to be infrequent in this region (upstream of the sequences corresponding to IL-7 GSP-2), because no nucleotide deletion was observed in any of the sequenced clones. As depicted in Fig. 3B, the 5' ends of longer fragments were located within the -601 to -515 region upstream of the translation start site (+1), while the 5' ends of shorter fragments were mapped within the -197 to -131 region. These results demonstrated that the human IL-7 gene is transcribed from

multiple transcription start sites that are clustered within two distinct regions approximately 300 to 500 bp apart from each other.

We then tested whether ~1.8- and ~2.4-kb IL-7 mRNAs might indeed differ in their 5' UTR stretches by Northern blot analysis using a 5' UTR probe corresponding to nucleotides at positions -539 to -242 (Fig. 2A). Interestingly, this probe exhibited subtle but substantial hybridization with ~2.4-kb but not with ~1.8-kb mRNA, showing the different lengths of 5' UTR between these mRNA species (Fig. 2B). To further confirm this, RT-PCR with any of the S primers (S1, S2, or S3) along with the AS1 primer (Fig. 2A) was carried out. When RNAs from untreated and IFN-γ-treated DLD-1 cells were examined, amplification with the primer sets of S3/AS1 and S2/AS1 showed no difference in the amount of products before and after IFN-γ treatment (Fig. 2C). In contrast, amplification with the primer set of S1/AS1 displayed a significant increase in the amounts of PCR products in response to IFN-γ (Fig. 2C). Therefore, it was demonstrated that stimulation with IFN-γ preferentially induces relatively short-form IL-7 mRNA expression via the selective usage of transcription initiation sites within the region -197 to -131. Of note, the maximum difference in 5' UTR lengths among clones obtained in RLM-RACE was less than 500 bp and did not match that between the ~2.4- and ~1.8-kb transcripts seen in Northern blot analysis. We assumed that this discrepancy might have in some part resulted from the difficulties in determining the precise size of transcripts by Northern blot analysis; however, this issue was not further examined in the present study.
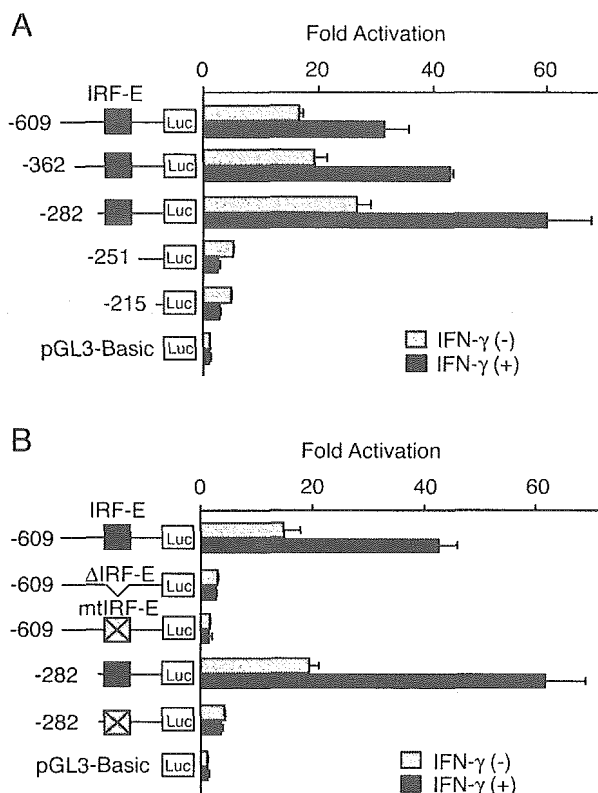
FIG. 4. IFN-γ-dependent and -independent IL-7 gene activation is mediated through IRF-E within its 5' UTR. (A) DLD-1 cells were transiently transfected with a −609-Luc or either of its 5' deletion mutant plasmids, cultured in the presence or the absence of IFN-γ for 12 h, and then assayed for reporter activities. (B) DLD-1 cells were transiently transfected with a −609-Luc or either of its mutated versions of plasmids, cultured as described for panel A, and then reporter activities were assayed. Luciferase activities were normalized and indicated as increases in activation compared with activity levels of cells transfected with pGL3-Basic plasmid and left untreated. Results are the means ± standard deviations of three independent experiments. Xs in boxes indicate mutated IRF-E sequences.

**IFN-γ-dependent and -independent IL-7 gene expression is mediated through IRF-E within its 5' UTR.** To characterize cis-acting regulatory elements in the 5' flanking or intragenic regions of the human IL-7 gene, we constructed a reporter plasmid in which the luciferase gene expression was under the control of the upstream region of the human IL-7 gene. When a reporter plasmid with the region −3194 to −3 (−3194-Luc) was transiently transfected in DLD-1 cells, a significant increase of luciferase activity was observed in both untreated and IFN-γ-treated cells, when compared to that seen with the control reporter plasmid (data not shown). A series of 5' deletions from the −3194-Luc to position −609 (−609-Luc) showed no apparent difference in reporter activities (data not shown), and, thus, we constructed another series of 5' deletion clones to be analyzed. As shown in Fig. 4A, the reporter activity of the −609-Luc was approximately 15-fold higher than that of the control in the absence of IFN-γ. In addition, the reporter activity exhibited approximately a twofold induction in response to IFN-γ. Deletions from the 5' end to −282 showed a slight increase in both basal and IFN-γ-inducible reporter activities. In contrast, further deletion up to position −251 re-

sulted in a dramatic decrease of reporter activities not only of uninduced levels but also with regard to IFN-γ-dependent induction (Fig. 4A). These results suggested that the critical enhancer element for both IFN-γ-dependent and -independent up-regulation of IL-7 gene expression might be located within the region from position −282 to −251. Substantial activities in the constitutive levels of reporter gene expression were observed further in the −215 to −3 region, while the IFN-γ-dependent induction of the reporter activity almost diminished by deleting up to position −251 (Fig. 4A). Since the region from position −282 to −251 contained an IRF-E at position −268 to −257 (Fig. 3B), we postulated that IL-7 gene activation might be mediated through this site. As expected, when an internal deletion mutant of the −282 to −251 sequence (−609-ΔIRF-E-Luc) was assayed, a drastic decrease in reporter activities in untreated as well as IFN-γ-treated cells was observed (Fig. 4B). In addition, introduction of a 4-bp mutation into the IRF-E sequences of −609-Luc and −282-Luc similarly culminated in a marked decrease in reporter activities (Fig. 4B). These findings suggested that the region from position −282 to −251 and, in particular, the IRF-E sequences within this region play a critical role in determining both IFN-γ-dependent and -independent enhancer activities in human IECs.

**IRF-1 is an inducible, while IRF-2 is a constitutive, binding protein to the IRF-E.** To identify nuclear factors that interact with the regulatory element of the IL-7 gene, we performed an EMSA by using a DNA probe corresponding to the sequences of the region −280 to −253. When nuclear extracts of DLD-1 and HT29-18N2 cells before and after IFN-γ addition were examined, several DNA-protein complexes were observed (Fig. 5A, C1 through C5). Among these, two (C2 and C5) displayed constitutive complex formation, and others (C1, C3, and C4) were induced by IFN-γ in both of these cell types (Fig. 5A, lanes 1 to 11). The formation of these complexes was sequence specific, since the nonlabeled DNA probe competed out the binding of nuclear proteins with the labeled probe (Fig. 5A, lane 13). In addition, a nonlabeled mutant probe did not affect complex formation, showing these complexes to be composed of proteins that specifically recognized IRF-E sequences (Fig. 5A, lane 14). Consistently, an anti-IRF-1 antibody shifted complex C3 (Fig. 5A, lanes 16 and 25), one of the inducible complexes in both cell types. In addition, complex C2, continuously observed with higher intensity in DLD-1 cells than in HT29-18N2 cells, was completely shifted with an anti-IRF-2 antibody (Fig. 5A, lanes 17 and 26). These observations were further supported by immunoblotting, since the nuclear expression of these IRF proteins correlated well with the results of the EMSA analysis (Fig. 5B). It should be noted that in the supershift experiments, nuclear complexes containing other IRF family proteins such as IRF-4, IRF-8, and IRF-9 were also present to some extent (Fig. 5A, lanes 19, 21, and 22). However, the degree of their occupancy on IRF-E sequences remained unclear, since antibodies against these molecules could neither shift nor disrupt the protein-DNA complexes. Together, these observations indicated that IRF-1 and IRF-2 bind to the IRF-E in an IFN-γ-inducible and constitutive manner, respectively, and then transcriptionally regulate IL-7 gene expression. Again, this notion showed an analogy with the previously described mechanisms of IL-7 gene transcription in
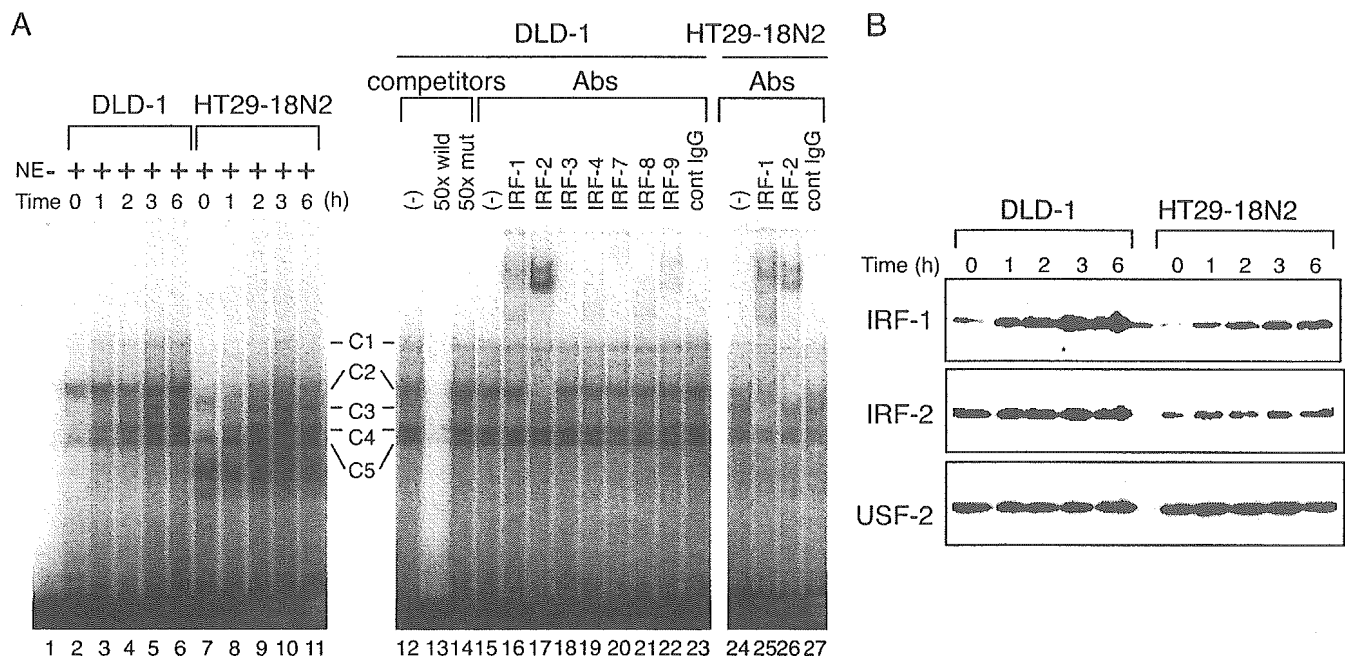
FIG. 5. IRF-1 is an inducible, while IRF-2 is a constitutive, binding protein to the IRF-E. (A) DLD-1 and HT29-18N2 cells were stimulated with IFN-γ (50 ng/ml) for the indicated time periods. Nuclear extracts (NE) were prepared, and 10 μg of each was subjected to EMSA by using $^{32}$P-labeled oligonucleotide probes corresponding to the sequence −280 to −253 of the IL-7 gene (left). Competition assays were performed by adding a 50-fold molar excess of unlabeled specific oligonucleotide (wild) or the mutant (mut) probe to the reaction mixture containing the extracts from cells treated with IFN-γ for 6 h (right). Supershift assays were performed by preincubating the reaction mixture of 6 h-treated nuclear extracts with either 2 μg of antibodies (Abs) against the indicated proteins or 2 μg of mouse IgG. (B) Twenty-five micrograms of nuclear extracts as described in panel A was separated on an SDS–10% polyacrylamide gel and immunoblotted with an anti-IRF-1 antibody (IRF-1), and the blot was sequentially reprobed with an anti-IRF-2 (IRF-2), and an anti-USF-2 antibody (USF-2, loading control).

murine keratinocytes in terms of the IFN-γ-inducible DNA binding of IRF-1 to IRF-E (2). Our data, however, raised the further possibility that IRF-2, generally known as a transcriptional repressor, also acts as a positive regulator of IL-7 gene expression, since the constitutive DNA binding and relative abundance of the IRF-2-containing nuclear complex in DLD-1 compared to HT29-18N2 cells, closely paralleled the levels of IL-7 mRNA expression.

**IRF-1 and IRF-2 distinctively up-regulate IL-7 protein production via IRF-E-mediated transcription.** Given these observations, we next analyzed the functional effects of IRF-1 and IRF-2 on IL-7 gene expression. To this end, a −609-Luc plasmid was cotransfected with an expression plasmid for either IRF-1 or IRF-2 into DLD-1 cells. Intriguingly, introduction of not only IRF-1 but also IRF-2 significantly enhanced the reporter activities (Fig. 6A). The effects of these IRF proteins were mediated via IRF-E, since neither IRF-1 nor IRF-2 affected gene expression from a mutant reporter plasmid (Fig. 6A). These results clearly showed that both IRF-1 and IRF-2 positively regulate expression of the IL-7 gene through IRF-E on its 5′ UTR.

To examine whether such transcriptional regulation leads to IL-7 protein production, we next assessed DLD-1-derived cells in which a gene encoding either IRF-1 or IRF-2 was stably transfected. Since several studies showed that IRF-1 suppresses and that IRF-2 promotes cellular proliferation, respectively (10), we employed the TET-on inducible system to achieve conditional expression of these IRF proteins, thereby excluding the possibilities that such growth-regulating func-

tions might affect the direct effects of IRF-mediated transcription. In our system, tagged IRF proteins were expressed upon the addition of DOX, which relieved the repressive effects of TR proteins. When each clone of DLD-1/TR/IRF-1-tag or DLD-1/TR/IRF-2-tag cells was examined, each IRF protein was efficiently induced upon DOX treatment (Fig. 6B). In addition, when analyzed by transient transfection of −609-Luc, both clones displayed marked enhancement of reporter activities in response to DOX, suggesting that these tagged IRF proteins are transcriptionally competent (data not shown). When the culture supernatants of these cells before and after the DOX addition were assayed for IL-7 by ELISA, a marked induction of IL-7 proteins was observed in both DLD-1/TR/IRF-1-tag and DLD-1/TR/IRF-2-tag cells but not in parental DLD-1 cells (Fig. 6C), indicating that activation of IRF-1 or IRF-2 could induce IL-7 protein production. We further took advantages of this system to examine how inducible expression of each IRF protein influences the profile of IL-7 mRNAs. Interestingly, when Northern blotting with the IL-7 CS probe was performed, DOX-dependent IRF-1 expression exclusively induced generation of ~1.8-kb IL-7 mRNA (Fig. 6D). In contrast, the expression of IRF-2 significantly enhanced the expression of both ~2.4- and ~1.8-kb IL-7 transcripts (Fig. 6D). These results not only demonstrated the up-regulatory functions of IRF-1 and IRF-2 on IL-7 gene expression but also further reinforced our hypothesis that IRF-1 is an inducible, while IRF-2 is a constitutive, regulator of IL-7 gene expression; that is, these data coincided with the observation that IFN-γ-dependent IRF-1 expression was followed by the predominant
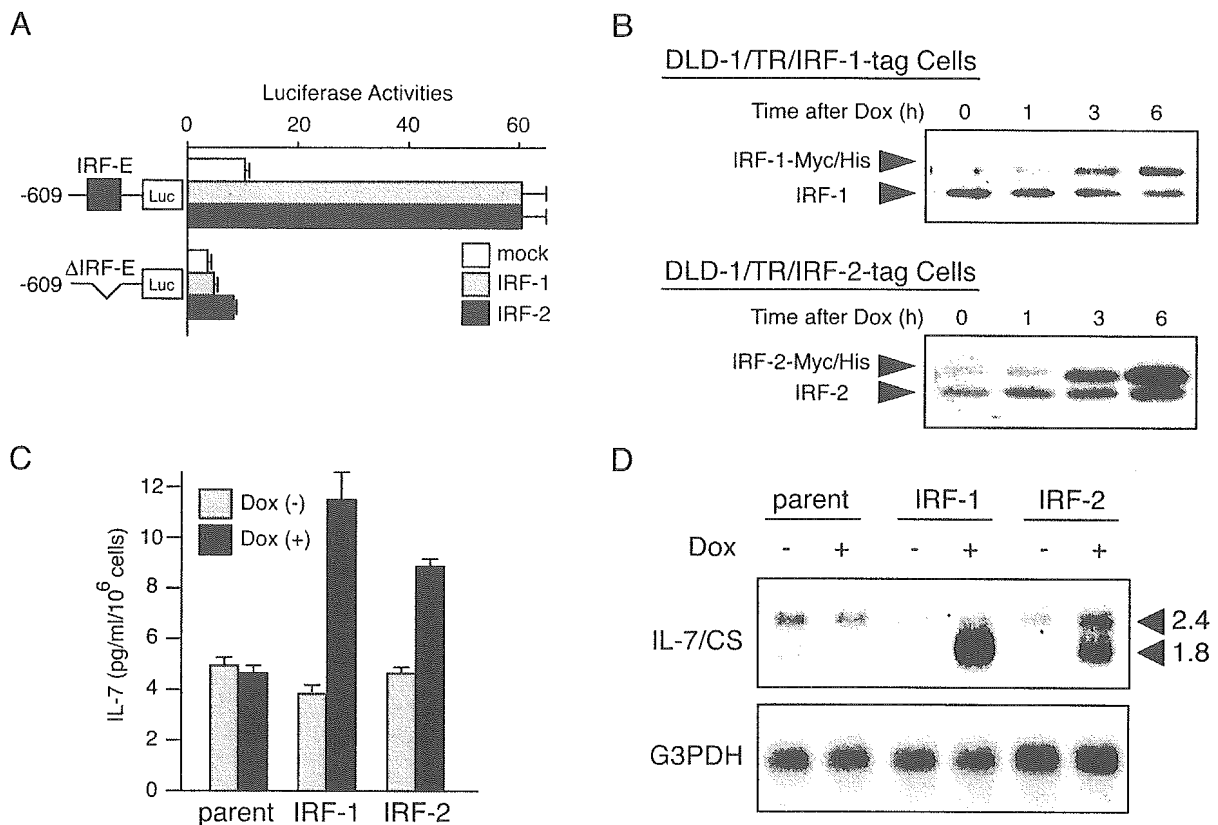
FIG. 6. IRF-1 and IRF-2 distinctively up-regulate IL-7 protein production via IRF-E-mediated transcription. (A) Either a −609-Luc plasmid or −609-mtIRF-E-Luc was transiently transfected into DLD-1 cells with 0.1 μg of the expression vector encoding either IRF-1 or IRF-2 (pcDNA3-IRF-1 or-IRF-2) or with an empty vector (mock). Cells were then cultured for 12 h and assayed for reporter activities. Luciferase activities were normalized and indicated as the means ± standard deviations of three independent experiments. (B) DLD-1-derived cells in which either IRF-1-tag or IRF-2-tag protein is inducible upon DOX were established. DLD-1/TR/IRF-1-tag and DLD-1/TR/IRF-2-tag cells were treated with DOX (100 ng/ml) for the indicated time periods. Nuclear extracts were prepared, and 25 μg of each was subjected to immunoblot analysis by using either anti-IRF-1 antibody for DLD-1/TR/IRF-1-tag cells or anti-IRF-2 antibody for DLD-1/TR/IRF-2-tag cells, respectively. (C) Parental DLD-1 (parent), DLD-1/TR/IRF-1-tag (IRF-1) and DLD-1/TR/IRF-2-tag (IRF-2) cells were treated with 100 ng of DOX (+) per ml or left untreated (−) for 24 h, and the supernatant was assayed for IL-7 production by ELISA. Results are the means ± standard deviations of three independent experiments. (D) Parental DLD-1 (parent), DLD-1/TR/IRF-1-tag (IRF-1) and DLD-1/TR/IRF-2-tag (IRF-2) cells were treated with DOX (100 ng/ml) and then collected at the time point of the addition (−) of IFN-γ or 6 h (+) after stimulation. Poly(A)[+] mRNA was extracted, and Northern blotting of IL-7 mRNA was performed as described in the legend of Fig. 2B by using a ^{32}P-labeled CS probe.

expression of ∼1.8-kb IL-7 mRNA, whereas constitutive IRF-2 expression was accompanied with the expression of both sizes of transcripts (Fig. 2B).

**Inducible and constitutive IL-7 production is suppressed by siRNAs for IRF-1 and IRF-2, respectively.** To clarify the distinct roles of IRF-1 and IRF-2 in IL-7 production directly, we designed siRNAs for either of these IRFs and then examined how these siRNAs affect IL-7 production. When DLD-1 cells were transiently transfected with either of the siRNAs, IFN-γ-dependent expression levels of IRF-1 and constitutive levels of IRF-2 were suppressed by 50 and 80% at the protein levels, respectively (Fig. 7A). In parallel, in cells treated with siRNA for IRF-1, IFN-γ-dependent IL-7 production was significantly inhibited by 50%, whereas constitutive IL-7 secretion was barely affected (Fig. 7B). In striking contrast, basal levels of IL-7 protein production in cells depleted of IRF-2 by specific siRNA were reduced by 40%, while these cells displayed an efficient induction of IL-7 secretion in response to IFN-γ (Fig. 7B). These data clearly demonstrated that IRF-1 functions as an inducible factor for IL-7 production, primarily in response

to cellular stimuli such as IFN-γ, while IRF-2 predominantly serves as a factor that maintains the constitutive levels of IL-7 production.

**IRF-1 and IRF-2 bind to the IRF-E without competition in vivo.** Our data showing the distinct functions of IRF-1 and IRF-2 on gene expression and the production of IL-7 raised the question of how the binding of each IRF to the IRF-E is regulated in vivo. To examine this, ChIP assays were performed with DLD-1 cell chromatin extracts. We designed two sets of PCR primers to amplify DNA fragments corresponding to the regions −539 to −159 and +976 to +1337 (positions on the genomic sequences relative to the translation start site), respectively (Fig. 8A). The former set of primers was used to amplify a fragment containing the IRF-E [IRF-E(+)] and the latter to amplify a distal genomic fragment within the intronic sequences more than 1.2 kb downstream of the IRF-E [IRF-E(-)]. As shown in Fig. 8B, anti-IRF-1 antibody precipitated only 0.03% of the IRF-E(+) DNA in total input chromatin in the absence of IFN-γ and, upon stimulation with IFN-γ, the levels of IRF-1 occupancy in this region significantly increased
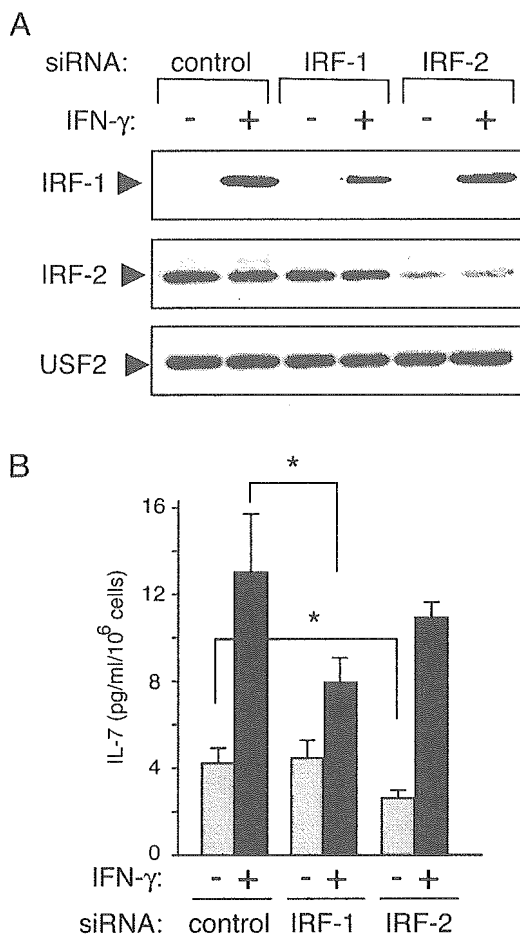
A



B



FIG. 7. Inducible and constitutive IL-7 production is suppressed by siRNAs for IRF-1 and IRF-2, respectively. DLD-1 cells were transfected with either siRNA duplex oligonucleotides targeting IRF-1, IRF-2, or control siRNA. After transfection, cells were cultured under the usual conditions for an additional 12 h, washed twice, and then cultured in the presence (+) or absence (−) of IFN-γ (50 ng/ml). The cells collected before (−) IFN-γ treatment and after 6 h (+) of IFN-γ treatment were subsequently subjected to immunoblotting (A) as described in the legend of Fig. 4B. In parallel, cells were identically treated as described for panel A, and the supernatants were collected after 24 h of culture in the presence (+) or the absence (−) of IFN-γ (B). Measurement of IL-7 was performed by ELISA, and results are indicated as the means ± standard deviations of three independent experiments. *, $P < 0.05$ by a paired Student $t$ test.

(0.6%) (Fig. 8B). By contrast, the binding of IRF-2 to the IRF-E remained unchanged before (0.11%) and after (0.10%) stimulation with IFN-γ (Fig. 8B). The specificity of immunoprecipitation with antibodies against each IRF protein was verified by the finding that the amounts of IRF-E(+) fragments in the immunoprecipitates by control antibodies were at significantly low levels (0.02% in both IFN-γ-untreated and -treated chromatins) (Fig. 8B). In addition, specific binding of IRF-1 and IRF-2 to the IRF-E was confirmed because immunoprecipitation of IRF-1 or IRF-2 recovered only a small amount of the genomic region located far downstream of the IRF-E [IRF-E(-)], while that of histone H3 recovered approximately 10% of the total input IRF-E(-) fragments (Fig. 8B). Since there may exist variations in cross-linking and immunoprecipitation efficiency between these IRF proteins, it seems

difficult to directly compare the absolute levels of promoter occupancy of these IRFs. However, from these observations, it was formally suggested that IRF-Es on the IL-7 genes are constitutively but not fully occupied by IRF-2, regardless of the
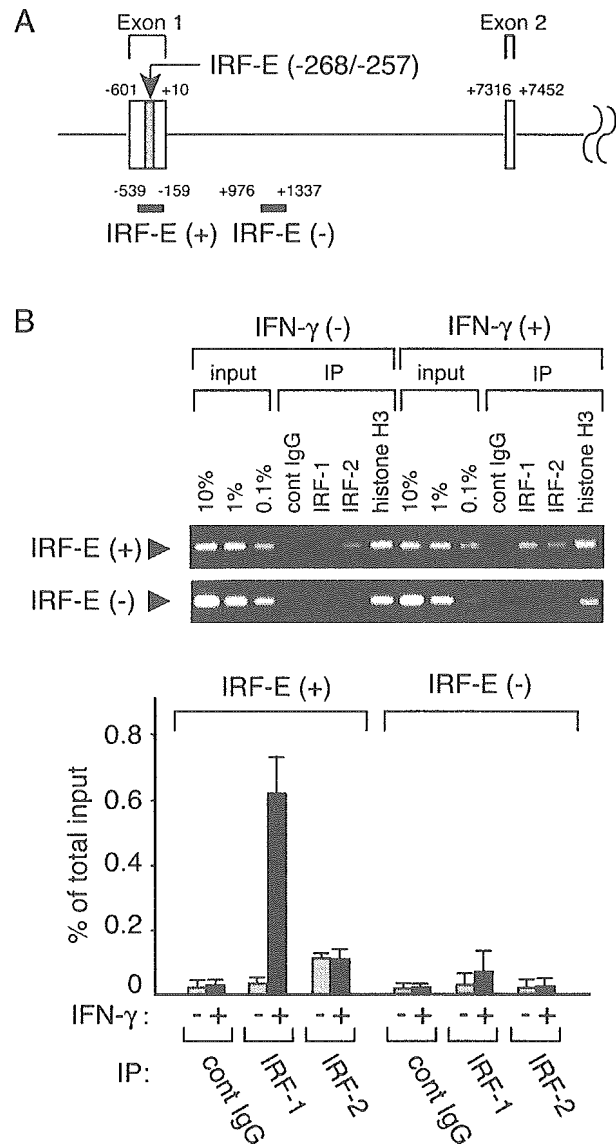
A



B



FIG. 8. IRF-1 and IRF-2 bind to IRF-E without mutual exclusion in vivo. (A) Schematic representation of the 5' part of the human IL-7 gene. Exon 1, 2, and the intervening intron are shown with the nucleotide number relative to the translation initiation site (+1). IRF-E located in exon 1 (shaded) and the DNA regions analyzed by ChIP assays [IRF-E(+) and IRF-E(-)] are also indicated. (B) DLD-1 cells were treated with IFN-γ or left untreated for 6 h and processed for ChIP assays by using anti-IRF-1, anti-IRF-2, and anti-histone H3 antibodies (positive control) or control Ig (negative control). Precipitated DNA was subjected to both conventional PCR (top) and quantitative PCR (bottom) to amplify either the IL-7 gene fragment (−539 to −159) containing the IRF-E on its 5' UTR [IRF-E(+)] or the intronic fragment (+976 to +1337) [IRF-E(-)]. The amount of immunoprecipitated IL-7 gene fragment relative to that present in total input chromatin (% of total input) was calculated as described in Materials and Methods. Data are shown as the means ± standard deviations of three independent chromatin immunoprecipitations (bottom). IP, immunoprecipitation; cont, control.
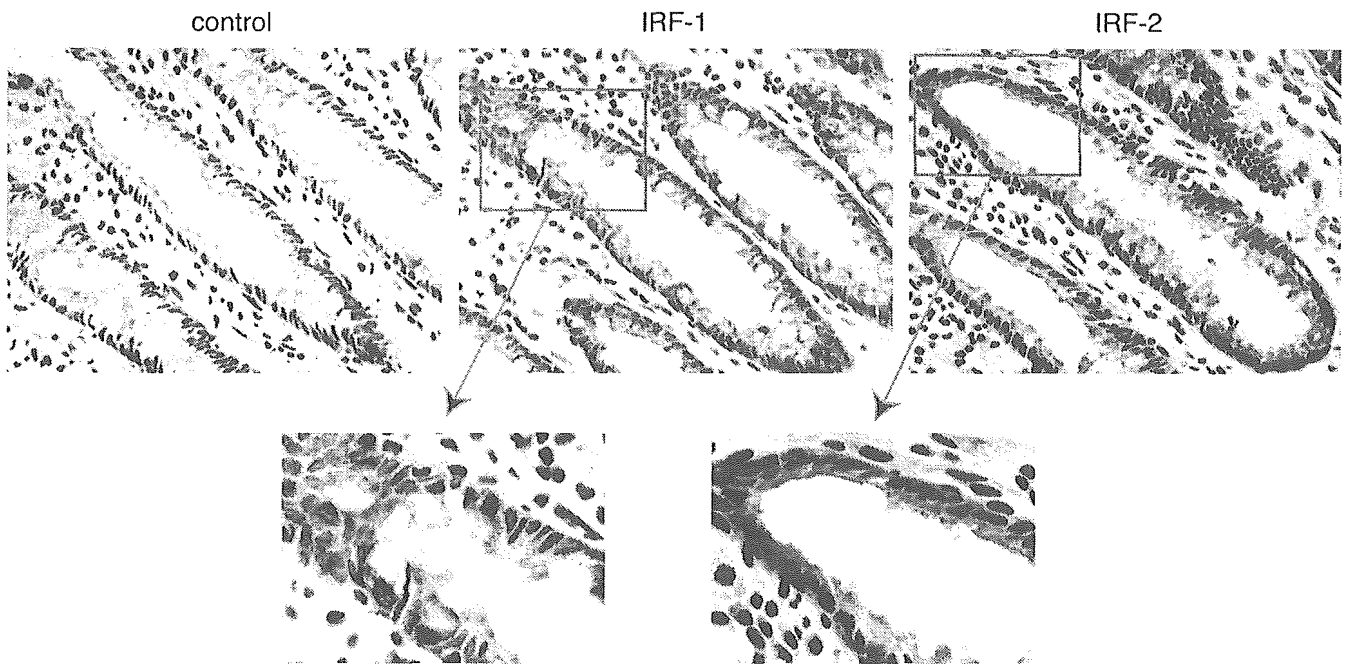
FIG. 9. IRF-1 and IRF-2 proteins are expressed in human colonic epithelial cells with distinct patterns of distribution. Sections of human colonic mucosal tissues were subjected to immunohistochemical analysis. Tissue sections (8 μm) were stained with either anti-IRF-1 (IRF-1), anti-IRF-2 (IRF-2) antibody, or purified rabbit IgG (control) (original magnification, ×400).

extracellular stimuli, and are further bound by IRF-1 upon stimulation with IFN-γ.

**IRF-1 and IRF-2 proteins are expressed in human colonic epithelial cells with distinct patterns of distribution.** Finally, to clarify the issue as to whether IRF-1 and IRF-2 proteins are physiologically expressed in human IECs in vivo, sections of adult human colonic tissues were immunostained with a specific antibody against IRF-1 or IRF-2. As shown in Fig. 9, both IRF proteins were expressed in colonic epithelial cells, as well as in nonepithelial cells in the lamina propria (Fig. 9). Furthermore, immunoreactivities against these factors preferentially exhibited nuclear patterns, indicating that these IRF proteins function as transcriptional regulators in human IECs in vivo. Interestingly, staining with anti-IRF-2 antibody distributed throughout the epithelial layer (Fig. 9). In contrast, IRF-1 was expressed with a patchy distribution, irrespective of the cellular configuration within the crypt (Fig. 9). Remarkably, most of the IRF-1-positive cells were shown to be epithelial goblet cells, as judged by their expanded shape at the apical portion (Fig. 9). We confirmed this finding by double staining with anti-IRF-1 antibody and acidic mucus staining with alcian blue on the same section (data not shown). These results indicated that both IRF-1 and IRF-2 proteins are expressed in colonic epithelial cells with quite distinct patterns of distribution. Moreover, together with our previous demonstration that IL-7 is substantially expressed throughout the epithelial layer, with the most abundant expression in the goblet cells (30), it was suggested that these distinct patterns of distribution might be associated with the diffuse but nonuniform expression of IL-7 in human IECs in vivo.

## DISCUSSION

Recent evidence has implicated the profound effects of IL-7 on developing and mature lymphocytes not only in systemic (6) but also in local immune regulations in humans. However, the mechanisms of IL-7 production in human tissue-derived cells have remained unclear. In this study, using human IEC lines, we investigated the molecular mechanisms of IL-7 production and showed that IRF-1 and IRF-2 serve as critical factors for gene expression and the production of IL-7. Furthermore, IRF-1 and IRF-2 were demonstrated to play different roles in this process, suggesting that the IL-7 production might be regulated via finely coordinated mechanisms mediated by these IRF proteins.

Concerning the potentials of various cellular stimuli to influence IL-7 production, IL-1, TNF-α, and TGF-β had no effect and only IFN-γ was capable of regulating IL-7 production from IECs. These findings contrasted to results obtained with other tissue-derived human cells, since previous studies revealed that IL-1 and TNF-α enhance (34), while TGF-β suppresses IL-7 production in BM stromal cells (27). It seems unlikely that human IECs failed to respond to IL-1, TNF-α, or TGF-β merely due to low expression levels of the specific receptors for each factor, because most of these cytokines were proved to induce multiple biological responses within the human IEC lines or their sublines examined in this study (4, 33, 35). In addition, because the influences of these cytokines on IL-7 expression in human IECs were quite similar to those observed in murine keratinocytes (3), we favor the idea that IL-7 production in human IECs may be regulated by a tissue-specific mechanism which differs at least from that in human

BM stromal cells but resembles that in murine keratinocytes. Although the mechanisms accounting for the diversity of IL-7 production in different cell types have remained unknown, it would be of importance to clarify this issue to understand a variety of biological functions exerted by IL-7 in systemic immune regulation in humans.

In this study, we demonstrated that the transcription of the human IL-7 gene begins from multiple sites distributed within two separate regions at positions −601 to −515 and −197 to −131 bp upstream of the translation start site. Utilization of many transcription start sites is frequently observed in the regulation of genes whose promoters lack common core promoter sequences (26). Consistent with this, analysis of the human IL-7 gene revealed that none of the consensus sequences for the canonical TATA box, the initiator element YYAN(T/A)YY, or the downstream core promoter element occur within or in the vicinity of the region −601 to +1 (Fig. 3B). Instead, as initially documented in an earlier report (18), the 5' flanking region of the human IL-7 gene displays an unusually high number of CpG dinucleotides within a ∼700-bp region. This is also in accordance with the fact that a number of promoters within CpG islands lack all these classes of core elements (26). In addition, recent studies identified a new class of promoter motif on several genes that utilize multiple start sites in their TATA-less promoters. This motif, called MED-1 (multiple start site element downstream), was defined as the sequence GCTCC(C/G) and was shown to lie 20 to 45 bp downstream of the multiple transcription initiation window of various TATA-less promoters (11). Interestingly, an identical sequence to MED-1 occurs on the human IL-7 gene at position −498 (Fig. 3B), 17 to 103 bp downstream of one of two separate windows of the IL-7 gene transcription start sites. The functional relevance of these promoter structures to the start site selection of the IL-7 gene has remained undetermined; however, our work provides evidence that the expression of human IL-7 is regulated through a unique and unusual promoter architecture.

In addition to the promoter structure, unusual features of regulatory mechanisms were also found in IL-7 gene transcription. We showed that, by use of TET-inducible expression systems for each IRF protein, IRF-1 selectively induces transcription of the IL-7 gene from the relatively downstream region, while IRF-2 up-regulates transcription from two regions both upstream and downstream of IRF-E. These results suggest that utilization of the aforementioned two separate promoters is regulated by distinct as well as overlapping properties of IRF-1 and IRF-2 via binding to the same IRF-E. Recently, growing evidence has revealed the existence of alternative promoters on various human genes, suggesting the regulatory roles of alternative promoter usages in tissue-specific or developmentally controlled gene expression (15). Among these, however, the mechanism of IL-7 gene regulation seems to be unique, because there has been no report of such a gene whose alternative promoter usage is regulated by the differential binding of transcription factors to a single cis-element so far. At this time, it remains unclear why IRF-2 simultaneously promotes transcription from two regions but IRF-1 does not. One possible explanation for the IRF-2-mediated dual promoter usage is that the binding of IRF-2 to the IRF-E might alter the chromatin architecture to a more relaxed configura-

tion than that of IRF-1. For example, it was shown that the proto-oncogene c-myc is transcribed from two distinct promoters that are located 160 bp apart, and an element called ME1a1, located between these two promoters, is required for the simultaneous opening of the chromatin configuration for both promoters (1). Therefore, it could be speculated that the IRF-E, like ME1a1 on the c-myc gene, might allow the transcription from two promoters only when it is bound by IRF-2 in conjunction with the specifically assembled transcription machinery.

Despite the alternative promoter usage, no variation in the resulting IL-7 proteins has been reported. Interestingly, as is the case with the murine IL-7 transcripts (8), human transcripts contain multiple potential initiation codons (nine in total throughout the −601 to −1 region) upstream from the authentic initiation codon (Fig. 3B). As these potential upstream sites generally decrease the translational efficiency (14) and as the removal of the 5' noncoding sequence improves the translational efficiency of murine IL-7 mRNA (23), it is postulated that the human IL-7 transcripts with a shorter 5' UTR might also be translationally more active than a transcript with a longer one.

In the present study, we demonstrated the physiological roles of IRF-1 and IRF-2 in IL-7 production by human IECs. IRF-1, originally identified as a transcriptional regulator for the human IFN-β gene (19), is induced upon various stimuli and activates target gene expression (9, 19). Likewise, we here showed that nuclear expression of IRF-1 and its binding to the IRF-E were also induced upon IFN-γ treatment in human IECs. These data recapitulated the mechanisms existing in murine keratinocytes, since it was shown that IFN-γ-dependent IL-7 gene expression was preceded by increased binding of IRF-1 to the IRF-E in these cells, and the inhibition of IRF-1 mRNA expression by UV light suppressed this IFN-γ-inducible IL-7 expression (2). In addition, our observations of DOX-inducible expression and siRNA-mediated suppression of IRF-1 were of importance, since these confirmed that such IRF-1-mediated transcription is indeed important for the inducible production of IL-7 protein. IRF-1 protein is substantially expressed with a patchy distribution in normal human intestinal epithelia, and the predominant expression of IRF-1 in goblet cells was consistent with the fact that relatively abundant expression of IL-7 is observed in these cells (30). Considering that IFN-γ is constitutively expressed in IELs (16), IRF-1 expression in vivo might be the result of the IFN-γ action that is locally produced from a certain type of cells such as IELs. Alternatively, expression of IRF-1 might be additionally regulated by stimuli other than IFN-γ, since IRF-1 is up-regulated by a variety of cellular stimuli such as various cytokines (7) and viral infection (19). At present, it is unclear which type of stimuli is responsible for IRF-1 expression in vivo and why goblet cells are prone to express IRF-1 proteins. However, our study provides not only the molecular basis accounting for the cell type-dependent variable expression of IL-7 in human IECs but also a clue for the better understanding of a well-coordinated network system within the intestinal mucosa: IL-7 production from IECs is regulated by sensing and responding to the immunological status such as the microenvironmental cytokine milieu, primarily utilizing IRF-1 as a transcriptional activator.

Although IRF-2 was originally described as a transrepressor with its potential for competing with IRF-1 (9), studies have shown that IRF-2 also functions as a transcriptional activator for several genes (12, 17, 28, 36). We here demonstrated that IRF-2 also acts as a transactivator for the IL-7 gene, but its up-regulatory functions in the production of IL-7 is quite different from those of IRF-1. Silencing IRF-2 expression by its specific siRNA resulted in suppression not of the IFN-γ-inducible but of the basal levels of IL-7 production, and DOX-regulated expression of IRF-2 enhanced IL-7 protein production via expression of both ~2.4- and ~1.8-kb IL-7 mRNAs that are constitutively expressed. Concerning the fact that IRF-2 was ubiquitously expressed throughout the epithelial layer of human colonic tissues, these findings strongly suggest that IRF-2, in contrast to IRF-1, serves as a critical regulator for IL-7 production from wide-ranging areas of human IECs in vivo. Furthermore, it was previously shown that IRF-1 is a short-lived protein with a half-life of about 30 min, while IRF-2 protein has a relatively longer half-life of more than 8 h (32). Given this, we may postulate that IRF-1 might act as a transient regulator of IL-7 production in response to cellular stimuli and, in contrast, that IRF-2 might serve as a critical factor to ensure the basal and steady-state levels of IL-7 production, not only at the cellular level but also in the tissue configuration within human intestinal mucosa.

We have previously reported that intestinal inflammation occurred in IL-7 transgenic mice (31). These mice spontaneously developed acute colitis at 1 to 3 weeks of age, which was followed by a chronic phase of colitis that histopathologically mimicked the human inflammatory bowel diseases. In these diseased mice, expression of IL-7 was increased in the acute phase while it was decreased in the chronic phase of colitis at the sites of inflammation (31). These results suggested that aberrant production of IL-7 might directly lead to the dysregulation of the local immune network in the intestinal mucosa. Based on these observations, the present study also raises the issue of a potential role of IRF proteins in human diseases such as inflammatory bowel disease. We indicated that physiological expression of IRF-1 in vivo was dominated in epithelial goblet cells, depletion of which is one of the most prominent features of ulcerative colitis in humans. Meanwhile, it is well known that the inflamed mucosa in Crohn's disease exhibit increased levels of proinflammatory cytokines including IFN-γ (25). Therefore, it is possible for us to speculate that functional alteration or a decrease in the number of goblet cells in ulcerative colitis or the altered local cytokine milieu in Crohn's disease might lead to the escape from appropriate function or expression of these IRF proteins in IECs, linking improper production of IL-7 to the dysregulation of mucosal lymphocytes within the sites of inflammation.

In summary, we here show that IRF-1 and IRF-2 serve as activators for IL-7 gene expression and protein production, while their respective roles are quite different. These results not only provide a molecular basis for understanding the profound functions of IEC-derived IL-7 in human intestinal mucosa but also suggest that the functional interplay between IRF-1 and IRF-2 is an exquisite mechanism that regulates the timely as well as continuous production of IL-7. We believe that the present work raises several interesting issues for further studies on the biological and pathological significance of these IRF proteins, especially in human IECs, in terms of their relationship with the pleiotropic functions of IL-7 in intestinal immune regulation.

## REFERENCES

1. Albert, T., J. Wells, J. O. Funk, A. Pullner, E. E. Raschke, G. Stelzer, M. Meisterernst, P. J. Farnham, and D. Eick. 2001. The chromatin structure of the dual c-myc promoter P1/P2 is regulated by separate elements. J. Biol. Chem. 276:20482–20490.
2. Aragane, Y., A. Schwarz, T. A. Luger, K. Ariizumi, A. Takashima, and T. Schwarz. 1997. Ultraviolet light suppresses IFN-gamma-induced IL-7 gene expression in murine keratinocytes by interfering with IFN regulatory factors. J. Immunol. 158:5393–5399.
3. Ariizumi, K., Y. Meng, P. R. Bergstresser, and A. Takashima. 1995. IFN-gamma-dependent IL-7 gene regulation in keratinocytes. J. Immunol. 154:6031–6039.
4. Bartke, T., D. Siegmund, N. Peters, M. Reichwein, F. Henkler, P. Scheurich, and H. Wajant. 2001. p53 upregulates cFLIP, inhibits transcription of NF-kappaB-regulated genes and induces caspase-8-independent cell death in DLD-1 cells. Oncogene 20:571–580.
5. Bilenker, M., A. I. Roberts, R. E. Brolin, and E. C. Ebert. 1995. Interleukin-7 activates intestinal lymphocytes. Dig. Dis. Sci. 40:1744–1749.
6. Fry, T. J., and C. L. Mackall. 2002. Interleukin-7: from bench to clinic. Blood 99:3892–3904.
7. Fujita, T., L. F. Reis, N. Watanabe, Y. Kimura, T. Taniguchi, and J. Vilcek. 1989. Induction of the transcription factor IRF-1 and interferon-beta mRNAs by cytokines and activators of second-messenger pathways. Proc. Natl. Acad. Sci. USA 86:9936–9940.
8. Goodwin, R. G., S. Lupton, A. Schmierer, K. J. Hjerrild, R. Jerzy, W. Clevenger, S. Gillis, D. Cosman, and A. E. Namen. 1989. Human interleukin 7: molecular cloning and growth factor activity on human and murine B-lineage cells. Proc. Natl. Acad. Sci. USA 86:302–306.
9. Harada, H., T. Fujita, M. Miyamoto, Y. Kimura, M. Maruyama, A. Furia, T. Miyata, and T. Taniguchi. 1989. Structurally similar but functionally distinct factors, IRF-1 and IRF-2, bind to the same regulatory elements of IFN and IFN-inducible genes. Cell 58:729–739.
10. Harada, H., M. Kitagawa, N. Tanaka, H. Yamamoto, K. Harada, M. Ishihara, and T. Taniguchi. 1993. Anti-oncogenic and oncogenic potentials of interferon regulatory factors-1 and -2. Science 259:971–974.
11. Ince, T. A., and K. W. Scotto. 1995. A conserved downstream element defines a new class of RNA polymerase II promoters. J. Biol. Chem. 270:30249–30252.
12. Jesse, T. L., R. LaChance, M. F. Iademarco, and D. C. Dean. 1998. Interferon regulatory factor-2 is a transcriptional activator in muscle where it regulates expression of vascular cell adhesion molecule-1. J. Cell Biol. 140:1265–1276.
13. Kanamori, Y., K. Ishimaru, M. Nanno, K. Maki, K. Ikuta, H. Nariuchi, and H. Ishikawa. 1996. Identification of novel lymphoid tissues in murine intestinal mucosa where clusters of c-kit+ IL-7R+ Thy1+ lympho-hemopoietic progenitors develop. J. Exp. Med. 184:1449–1459.
14. Kozak, M. 1984. Selection of initiation sites by eucaryotic ribosomes: effect of inserting AUG triplets upstream from the coding sequence for preproinsulin. Nucleic Acids Res. 12:3873–3893.
15. Landry, J. R., D. L. Mager, and B. T. Wilhelm. 2003. Complex controls: the role of alternative promoters in mammalian genomes. Trends Genet. 19:640–648.
16. Lundqvist, C., S. Melgar, M. M. Yeung, S. Hammarstrom, and M. L. Hammarstrom. 1996. Intraepithelial lymphocytes in human gut have lytic potential and a cytokine profile that suggest T helper 1 and cytotoxic functions. J. Immunol. 157:1926–1934.
17. Luo, W., and D. G. Skalnik. 1996. Interferon regulatory factor-2 directs transcription from the gp91phox promoter. J. Biol. Chem. 271:23445–23451.
18. Lupton, S. D., S. Gimpel, R. Jerzy, L. L. Brunton, K. A. Hjerrild, D. Cosman, and R. G. Goodwin. 1990. Characterization of the human and murine IL-7 genes. J. Immunol. 144:3592–3601.
19. Miyamoto, M., T. Fujita, Y. Kimura, M. Maruyama, H. Harada, Y. Sudo, T. Miyata, and T. Taniguchi. 1988. Regulated expression of a gene encoding a

nuclear factor, IRF-1, that specifically binds to IFN-beta gene regulatory elements. Cell 54:903–913.

20. Monteleone, G., T. Parrello, F. Luzza, and F. Pallone. 1998. Response of human intestinal lamina propria T lymphocytes to interleukin 12: additive effects of interleukin 15 and 7. Gut 43:620–628.

21. Moore, T. A., U. von Freeden-Jeffry, R. Murray, and A. Zlotnik. 1996. Inhibition of gamma delta T cell development and early thymocyte maturation in IL-7 ⁻/⁻ mice. J. Immunol. 157:2366–2373.

22. Nakamura, T., R. Ouchida, T. Kodama, T. Kawashima, Y. Makino, N. Yoshikawa, S. Watanabe, C. Morimoto, T. Kitamura, and H. Tanaka. 2002. Cytokine receptor common beta subunit-mediated STAT5 activation confers NF-kappa B activation in murine proB cell line Ba/F3 cells. J. Biol. Chem. 277:6254–6265.

23. Namen, A. E., S. Lupton, K. Hjerrild, J. Wignall, D. Y. Mochizuki, A. Schmierer, B. Mosley, C. J. March, D. Urdal, and S. Gillis. 1988. Stimulation of B-cell progenitors by cloned murine interleukin-7. Nature 333:571–573.

24. Orlando, V. 2000. Mapping chromosomal proteins in vivo by formaldehyde-crosslinked-chromatin immunoprecipitation. Trends Biochem. Sci. 25:99–104.

25. Podolsky, D. K. 2002. Inflammatory bowel disease. N. Engl. J. Med. 347:417–429.

26. Smale, S. T., and J. T. Kadonaga. 2003. The RNA polymerase II core promoter. Annu. Rev. Biochem. 72:449–479.

27. Tang, J., B. L. Nuccie, I. Ritterman, J. L. Liesveld, C. N. Abboud, and D. H. Ryan. 1997. TGF-beta down-regulates stromal IL-7 secretion and inhibits proliferation of human B cell precursors. J. Immunol. 159:117–125.

28. Vaughan, P. S., F. Aziz, A. J. van Wijnen, S. Wu, H. Harada, T. Taniguchi, K. J. Soprano, J. L. Stein, and G. S. Stein. 1995. Activation of a cell-cycle-regulated histone gene by the oncogenic transcription factor IRF-2. Nature 377:362–365.

29. von Freeden-Jeffry, U., P. Vieira, L. A. Lucian, T. McNeil, S. E. Burdach, and

R. Murray. 1995. Lymphopenia in interleukin (IL)-7 gene-deleted mice identifies IL-7 as a nonredundant cytokine. J. Exp. Med. 181:1519–1526.

30. Watanabe, M., Y. Ueno, T. Yajima, Y. Iwao, M. Tsuchiya, H. Ishikawa, S. Aiso, T. Hibi, and H. Ishii. 1995. Interleukin 7 is produced by human intestinal epithelial cells and regulates the proliferation of intestinal mucosal lymphocytes. J. Clin. Invest. 95:2945–2953.

31. Watanabe, M., Y. Ueno, T. Yajima, S. Okamoto, T. Hayashi, M. Yamazaki, Y. Iwao, H. Ishii, S. Habu, M. Uehira, H. Nishimoto, H. Ishikawa, J. Hata, and T. Hibi. 1998. Interleukin 7 transgenic mice develop chronic colitis with decreased interleukin 7 protein accumulation in the colonic mucosa. J. Exp. Med. 187:389–402.

32. Watanabe, N., J. Sakakibara, A. G. Hovanessian, T. Taniguchi, and T. Fujita. 1991. Activation of IFN-beta element by IRF-1 requires a posttranslational event in addition to IRF-1 synthesis. Nucleic Acids Res. 19:4421–4428.

33. Weaver, S. A., M. P. Russo, K. L. Wright, G. Kolios, C. Jobin, D. A. Robertson, and S. G. Ward. 2001. Regulatory role of phosphatidylinositol 3-kinase on TNF-alpha-induced cyclooxygenase 2 expression in colonic epithelial cells. Gastroenterology 120:1117–1127.

34. Weitzmann, M. N., S. Cenci, L. Rifas, C. Brown, and R. Pacifici. 2000. Interleukin-7 stimulates osteoclast formation by up-regulating the T-cell production of soluble osteoclastogenic cytokines. Blood 96:1873–1878.

35. Wilson, L., C. Szabo, and A. L. Salzman. 1999. Protein kinase C-dependent activation of NF-kappaB in enterocytes is independent of IkappaB degradation. Gastroenterology 117:106–114.

36. Xi, H., B. Goodwin, A. T. Shepherd, and G. Blanck. 2001. Impaired class II transactivator expression in mice lacking interferon regulatory factor-2. Oncogene 20:4219–4227.

37. Yokota, T., N. Sakamoto, N. Enomoto, Y. Tanabe, M. Miyagishi, S. Maekawa, L. Yi, M. Kurosaki, K. Taira, M. Watanabe, and H. Mizusawa. 2003. Inhibition of intracellular hepatitis C virus replication by synthetic and vector-derived small interfering RNAs. EMBO Rep. 4:1–7.

# CD4$^+$CD25$^{bright}$ T Cells in Human Intestinal Lamina Propria as Regulatory Cells[1]

Shin Makita,* Takanori Kanai,[2]* Shigeru Oshima,* Koji Uraushihara,* Teruji Totsuka,* Taisuke Sawada,* Tetsuya Nakamura,* Kazutaka Koganei,† Tsuneo Fukushima,† and Mamoru Watanabe*

It is well known that immune responses in the intestine remain in a state of controlled inflammation, suggesting that not only active suppression by regulatory T cells plays an important role in the normal intestinal homeostasis, but also its dysregulation leads to the development of inflammatory bowel disease. In this study, we demonstrate that the CD4$^+$CD25$^{bright}$ T cells reside in the human intestinal lamina propria (LP) and functionally retain regulatory activities. All human LP CD4$^+$ T cells regardless of CD25 expression constitutively expressed CTLA-4, glucocorticoid-induced TNFR family-related protein, and *Foxp3* and proliferate poorly. Although LP CD4$^+$CD25$^-$ T cells showed an activated and anergic/memory phenotype, they did not retain regulatory activity. In LP CD4$^+$CD25$^+$ T cells, however, cells expressing CD25 at high levels (CD4$^+$CD25$^{bright}$) suppressed the proliferation and various cytokine productions of CD4$^+$CD25$^-$ T cells. LP CD4$^+$CD25$^{bright}$ T cells by themselves produced fewer amounts of IL-2, IFN-$\gamma$, and IL-10. Interestingly, LP CD4$^+$CD25$^{bright}$ T cells with regulatory T activity were significantly increased in patients with active inflammatory bowel disease. These results suggest that CD4$^+$CD25$^{bright}$ T cells found in the normal and inflamed intestinal mucosa selectively inhibit the host immune response and therefore may contribute to the intestinal immune homeostasis. *The Journal of Immunology,* 2004, 173: 3119–3130.

T he gastrointestinal tract is home to the largest number of leukocytes in the body as well as being the site where these cells encounter abundant exogenous stimuli. Despite this potential immune stimulus, it is well known that immune responses in the intestine remain in a state of controlled inflammation (1). Regulation of the immune response here is a balance between the need to mount protective immunity toward pathogens while not activating damaging inflammatory responses to the plethora of harmless Ags present, including those derived from resident bacteria (2–4). To maintain the intestinal homeostasis, including immunological tolerance, functionally distinct subsets have been clearly defined in T cells (5, 6). Among these subsets, the regulatory T (T$_R$)[3] cell subset down-regulates immune responses for both foreign and self-Ags and effectively participates in the suppression of autoimmune disorders (7–9). The importance

of an intact immune system for the intestinal homeostasis is revealed by the fact that a number of immune manipulations, including deletion of cytokine genes and alterations in T$_R$ subsets, lead to the development of an animal model of inflammatory bowel disease (IBD) (10–12). Evidence emerging from these studies suggests that pathogenic responses in the intestine are derived by resident bacteria and are controlled by a functionally specialized population of T$_R$ cells in the GALT (13).

A variety of T$_R$ cells that display regulatory function in vitro or in vivo have been described. These can be subdivided into different subsets based on the expression of cell surface markers, production of cytokines, and mechanisms of action. Recent studies focused on CD25 as the best marker for CD4$^+$ T$_R$ cells in mice and humans (14–16). CD4$^+$CD25$^+$ T cells, which constitute ~10% of peripheral murine and human CD4$^+$ T cells, express CTLA-4 (17–20), glucocorticoid-induced TNFR family-related protein (GITR) (21, 22), and the forkhead/winged helix transcription factor *Foxp3* (23–25). Although autoimmune diseases, including IBD, can be induced by reconstituting immunodeficient mice with peripheral CD4$^+$ T cells, which have been depleted of CD4$^+$CD25$^+$ (26) or CD4$^+$GITR$^+$ T cells (27), not only the existence of human intestinal CD4$^+$CD25$^+$ T$_R$ cells in normal or diseased condition but also their role in the pathogenesis of IBD are largely unknown. Conversely, several findings, for example. the evidence of the accumulated CD25$^+$, CD69$^+$, and CD71$^+$ (transferrin receptor) cells, indicate an increased state of activation of the T cell system in IBD (28). Although intestinal lamina propria (LP) T cells are already preactivated, the activation is further increased in both the circulation and mucosa from IBD patients as determined by several activation markers as compared with those from normal individuals (29). Furthermore, this activated phenotype is increased in involved compared with uninvolved areas or control tissue (29), being so far believed that these activated CD4$^+$CD25$^+$ cells should be pathogenic for the development of IBD. These conflicting findings prompted us to determine whether or not the LP

CD4$^+$CD25$^+$ T cells in IBD patients were pathogenic (effector) or protective (T$_R$) in this study.

Furthermore, there is much other evidence showing that 1) the peripheral CD4$^+$CD25$^-$ T cell population also possesses some regulatory activity (26, 30–34), 2) anergic/memory T cells have regulatory properties (35–38), and 3) LP CD4$^+$ T lymphocytes, regardless of CD25 expression, are generally memory T cells, and hyporesponsive to TCR-mediated proliferative signals (39, 40), indicating these cells could be highly differentiated effector or effector memory T cells (41, 42) with a raised threshold of activation that prevents immune responses to harmless intraluminal Ags.

In the present study, we investigate the existence and the role of the human LP CD4$^+$CD25$^{bright}$ as well as CD4$^+$CD25$^+$ and CD4$^+$CD25$^-$ T cells. We demonstrate here that human LP CD4$^+$ T cells from the normal intestine, regardless of CD25 expression, express other regulatory markers, CTLA-4, GITR, and *Foxp3*, and show anergic and memory features, but only CD4$^+$CD25$^{bright}$ LP T cells retain T$_R$ function, which can mediate potent suppression of autologous T cell proliferation and various cytokine productions, such as IFN-$\gamma$ and IL-2. Furthermore, we show here that these T$_R$ cells are significantly increased in patients with active IBD.

## Materials and Methods

### Patients and samples

Normal mucosal samples were obtained from macroscopically and microscopically unaffected areas of 54 colonic specimens from patients with colon cancer who underwent surgery and were obtained from the surgical resected samples of intestinal inflamed mucosa of 24 patients with colonic type Crohn's disease (CD) and 25 patients with ulcerative colitis (UC). The mucosa was prepared immediately after stripping away the underlying submucosa by blunt dissection. All experiments were approved by the Committee on Human Subjects of both Tokyo Medical and Dental University Hospital (Tokyo, Japan) and Yokohama City Hospital (Yokohama, Japan). Informed consent was obtained from all patients before the study. Disease activity in each patient with CD was analyzed according to the Crohn's Disease Activity Index and endoscopic and histopathological data. The disease had been present from 6 mo to 15 years. When the experimental study was performed in patients with CD, 4 patients were taking only steroids, 4 were taking both steroids and sulfasalazine, 3 were receiving both azathioprine and sulfasalazine, 11 were taking only sulfasalazine, and 2 had been undergoing nonspecific therapy for the previous 3 mo. In the UC group, disease activity was defined by the Truelove-Witts criteria and endoscopic (Matts grade) and histopathological data. When the experimental study was performed, 1 patient was receiving only steroids, 14 were receiving both steroids and sulfasalazine, 6 were taking only sulfasalazine, 3 were receiving azathioprine, steroids and sulfasalazine, and 1 patient had been undergoing nonspecific treatment for at least 3 mo.

### Culture media, reagents, and Abs

In all in vitro assays, cells were cultured in RPMI 1640 medium supplemented with 2 mM L-glutamine, 100 IU/ml penicillin/100 $\mu$g/ml streptomycin (Sigma-Aldrich, St. Louis, MO), 2 × 10$^{-5}$ M 2-ME, and 10% FCS (Invitrogen, Carlsbad, CA).

The following mAbs were used for purification of cell populations and flow cytometry analysis: RPA-T4, FITC- and Cy-Chrome-conjugated anti-human CD4; M-A251, PE-conjugated anti-human CD25; HI100, PE-conjugated anti-human CD45RA; UCHL1, PE-conjugated anti-human CD45RO; G46-6, PE-conjugated anti-HLA-DR; M-A712, PE-conjugated anti-human CD71;

BNI3, PE-conjugated anti-CTLA-4; MQ1-17, PE-conjugated anti-IL-2; JES3-19F1, PE-conjugated anti-IL-10; 4S.B3, PE- and FITC-conjugated anti-IFN-$\gamma$ (BD Pharmingen, San Diego, CA); 110416, PE-conjugated anti-human GITR (R&D Systems, Minneapolis, MN).

Purified recombinant human IL-2 (rhIL-2; kindly provided by Shionogi Pharmaceutical, Osaka, Japan), purified anti-human CD3 mAb (HIT3a; BD Pharmingen), Con A (Sigma-Aldrich), PHA (Sigma-Aldrich), and mitomycin C (MMC, Sigma-Aldrich) were used for in vitro coculture assay.

### Isolation of LP mononuclear cells (LPMCs) from intestinal mucosa

LPMCs were isolated from surgically resected intestinal specimens using enzymatic techniques as previously described (43). Briefly, the dissected mucosa was incubated in calcium and magnesium-free HBSS containing 2.5% FBS and 1 mM DTT (Sigma-Aldrich) to remove mucus. The mucosa was then incubated in medium containing 0.75 mM EDTA (Sigma-Aldrich) for 60 min at 37°C. During this treatment, intraepithelial lymphocytes and epithelial cells were released from the tissue and tissues containing LPMCs were collected and incubated in medium containing 0.02% collagenase (Worthington Biochemical, Freehold, NJ). The fraction was pelleted twice through a 40% isotonic percoll solution and the cells were then centrifuged over a Ficoll-Hypaque density gradient (40% and 60%). The purity of resulting LPMCs was analyzed by flow cytometry.

The CD4$^+$ T cells from LPMCs and PBMCs were purified by positive selection with the CD4$^+$ MultiSort kit (Miltenyi Biotec, Auburn, CA) (27). The MMC-treated CD4$^-$ fraction was used as APCs in the following experiments. The CD4$^+$CD25$^-$, CD4$^+$CD25$^+$, and CD4$^+$CD25$^{bright}$ populations were isolated from LPMCs and PBMCs by sorting using a FACSVantage (BD Biosciences, San Jose, CA) in accordance with the method by Baecher-Allan et al. (44), who demonstrated that the regulatory CD4$^+$ T cells in PBMCs of healthy human subjects preferentially reside within the CD4$^+$CD25$^{bright}$ T cell population. Cells were incubated with FITC-conjugated anti-CD4 and PE-conjugated anti-CD25 mAbs. The analysis and sort gates were restricted to the population of lymphocytes by means of their forward and side scatter properties. Large, activated T cells were excluded. On reanalysis, the forward and side scatter properties of the CD4$^+$CD25$^{bright}$ cells were not appreciably different from those of the CD4$^+$CD25$^-$ population, indicating that these cell populations are similar in size. In another set of experiments, LPMCs were stained with CyChrome-anti-CD4, FITC-anti-CD25, and PE-anti-CD45RO or PE-anti-CD71 mAbs, and the various subsets of cells were purified by a FACSVantage. For polyclonal activation, cells were cultured with 5 $\mu$g/ml plate-bound anti-CD3 (UCHT1; BD Pharmingen) and 5 $\mu$g/ml soluble anti-CD28 (CD28.2; BD Pharmingen) for 48 h and used for FACS and RT-PCR analyses.

### FACS analysis of surface and intracellular Ags

For two-color flow cytometry analysis, freshly isolated LPMCs and PBMCs were stained with FITC-conjugated anti-CD4 and PE-conjugated anti-CD25 (27). For three-color flow cytometry analysis, the samples stained with CyChrome-conjugated anti-CD4 and FITC-conjugated anti-CD25 were also stained with control PE-IgG1, or PE-conjugated CD45RO, PE-conjugated anti-CD45RA, PE-conjugated anti-HLA-DR, or PE-conjugated anti-GITR mAb. Before staining with PE-conjugated anti-CTLA-4 mAb, the cells were fixed and permeabilized with Cytofix/Cytoperm (BD Pharmingen) at 4°C for 30 min. Staining and washing were performed in Perm/Wash Buffer (BD Pharmingen), and cells were washed

once in PBS before analysis. For GITR staining, the sorted CD4$^+$CD25$^-$ and CD4$^+$CD25$^{bright}$ cells stimulated with anti-CD3/CD28 mAbs were also used.

### Cell stimulation assays

The CD4$^+$CD25$^-$ cells were plated at $1.0 \times 10^4$/well, while the CD4$^+$CD25$^{bright}$ cells were plated at $0, 0.5 \times 10^4$, or $1.0 \times 10^4$/well (27). Thus, upon coculture, the cells were combined at various ratios of $T_R$ responder in 96-well round-bottom plates (Corning Costar, Cambridge, MA) in the presence or absence of Con A (5 $\mu$g/ml), PHA (5 $\mu$g/ml), or soluble anti-CD3 mAb (1 $\mu$g/ml). To evaluate the effect of IL-2 on the break of anergy, cells were cultured with soluble anti-CD3 (1 $\mu$g/ml) in the presence or absence of rhIL-2 (100 U/ml). To assess a role of suppressive activity via competition between $T_R$ cells and responder cells for IL-2, various concentrations of rhIL-2 (0, 2, 5, 10, or 100 U/ml) were added. All wells received $5 \times 10^4$ MMC-treated CD4$^-$ cells as APCs. To determine proliferation, 50 $\mu$l of the culture supernatant was removed from each before 1 $\mu$Ci of [$^3$H]thymidine (NEN, Boston, MA) was added on day 3, the final 9 h of culture before harvesting. Percent proliferation was determined as (cpm incorporated in the coculture)/(cpm of responder population alone) $\times$ 100%.

### Cytokine assays

Intracytofluorimetric analysis of IL-2, IL-10, and IFN-$\gamma$ synthesis at the single-cell level was performed. Briefly, $1 \times 10^6$ cells were stimulated with 5 ng/ml PMA plus 500 nM ionomycin for 6 h, the last 4 of which was in the presence of 5 $\mu$g/ml brefeldin A (Gol-giPlug; BD Pharmingen). Cells were collected, washed, fixed, and saponin permeabilized (Cytofix/Cytoperm; BD Pharmingen) and stained with cytokine-specific mAbs or isotype. In another set of experiments, the supernatants, which were removed before addition of [$^3$H]thymidine at proliferation assays, were diluted and analyzed by a cytometric bead array (Th1/Th2 Cytokine CBA 1; BD Pharmingen) according to the manufacturer's instructions.

### RT-PCR for the detection of Foxp3

Total cellular RNA was extracted from $5 \times 10^5$ freshly sorted CD4$^+$CD25$^-$ and CD4$^+$CD25$^{bright}$ cells and those stimulated with anti-CD3/CD28 mAbs using the RNeasy Mini kit (Qiagen, Valencia, CA), and yield was estimated spectrophotometrically. One hundred fifty nanograms of the total RNA was reverse transcribed using the Superscript First-Strand Synthesis System (Invitrogen). Foxp3 levels were measured by dual-labeled probe RT-PCR using Smart Cycler (Cepheid, Sunnyvale, CA). The PCR contained 0.3 mM of each primer, 0.2 mM probe, 3 mM MgCL$_2$ and 0.75 U of Platinum Taq polymerase (Invitrogen). The primer sequences were designed to bracket an intron to avoid amplification of genomic DNA (45). Their sequences were as follows; Foxp3 primers: 5'-TTCATGCACCAGCTCTCAACGG-3' and 5'-TCGTCCATCC TCCTTTCCTTGATC-3' (Sawader, Tokyo, Japan). PCR cycling conditions consisted of 95°C for 6 min, followed by 45 cycles of 95°C for 15 s, 60°C for 30 s, and 72°C for 30 s. Cycle threshold (CT) values were compared against a standard curve to estimate starting amounts of mRNA, and the relative expression of Foxp3 mRNA between samples was estimated by normalizing these values against 18S rRNA CT values were generated using a preoptimized 18S rRNA primer and probe set (Applied Biosystems, Foster City, CA).

### Statistical analysis

The results were expressed as the mean $\pm$ SD. Groups of data were compared by Mann-Whitney $U$ test. Differences were considered to be statistically significant when $p < 0.05$.

## Results

### Phenotypical properties of human CD4$^+$CD25$^+$ and CD4$^+$CD25$^-$ LP T cells

Paired samples of PBMCs and LPMCs from 15 individuals were analyzed by flow cytometry for the presence of the CD4$^+$CD25$^+$ T cells. Consistent with previous reports describing human naturally occurring CD4$^+$CD25$^+$ $T_R$ cells (44, 46-49), a total of $6.0 \pm 0.5\%$ of the peripheral blood (PB) CD4$^+$ T cells were CD25$^+$ (Fig. 1, A and B). Similarly, $6.4 \pm 0.6\%$ of the LP CD4$^+$ T cells was also CD25$^+$ (Fig. 1, A and B). In addition, the mean fluorescence intensity (MFI) of LP CD4$^+$CD25$^+$ T cells is similar to that of the PB CD4$^+$CD25$^+$ T cells (data not shown). Since it has been recently reported that both naturally occurring CD4$^+$CD25$^+$ $T_R$
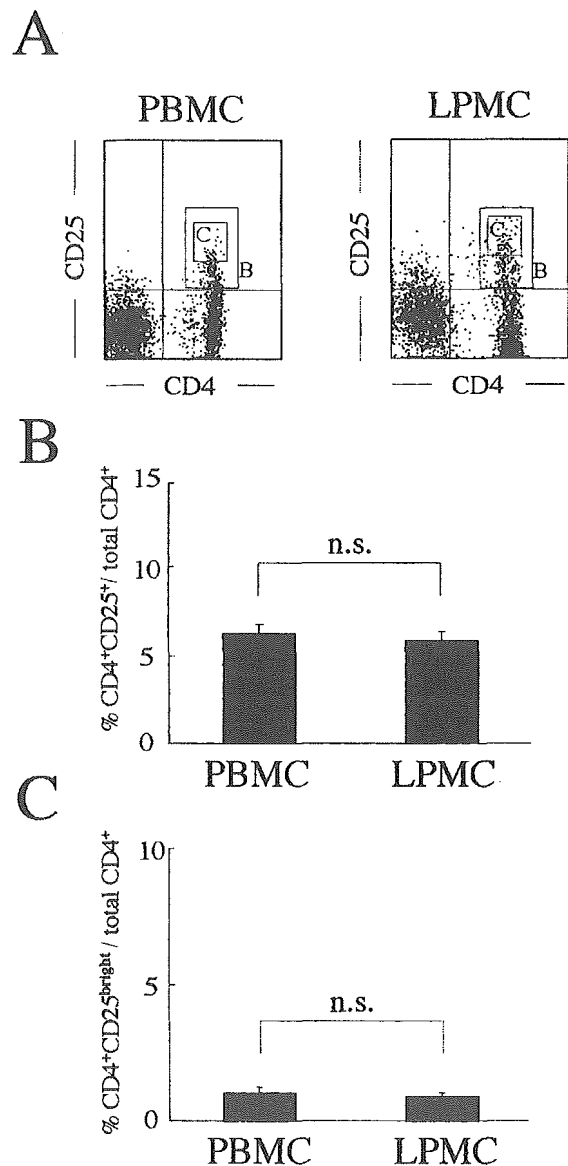


FIGURE 1. Identification of the PB and LP CD4$^+$CD25$^+$ and CD4$^+$CD25$^{bright}$ T cells. A, Freshly isolated human PBMCs and LPMCs were assessed by a FACSCalibur. Representative sorting gates of the three cell populations, CD25$^-$, CD25$^+$ (CD25$^{int}$ plus CD25$^{bright}$), and CD25$^{bright}$ are shown. B, The percentages of the PB and LP whole CD4$^+$CD25$^+$ T cells in total CD4$^+$ cells isolated from normal individuals ($n = 15$) was determined by a FACSCalibur. C, The percentages of the PB and LP CD4$^+$CD25$^{bright}$ T cells in total CD4$^+$ cells isolated from normal individuals ($n = 15$) was determined by a FACSCalibur.

cells (44, 50, 51) and anergic memory T$_R$ cells (52) preferentially resided in the CD4$^+$CD25$^{bright}$ T cell population in humans, we subdivided the CD4$^+$CD25$^+$ T cells into CD4$^+$CD25$^{bright}$ and CD4$^+$CD25$^{int}$ T cells. Also, 1.06 ± 0.23% and 0.90 ± 0.16% of the PB and the LP CD4$^+$ T cells, respectively, were CD4$^+$CD25$^{bright}$ (Fig. 1C), indicating that the LP CD4$^+$ T cells also may contain T$_R$ cells as well.

The PB and the LP CD4$^+$CD25$^-$, CD4$^+$CD25$^+$, and CD4$^+$CD25$^{bright}$ T cells were next analyzed for expression of surface Ags to gain insight into their mechanism of action and to more fully characterize the T$_R$ population in human intestinal LP. Consistent with previous reports (53), CD45RO, which can be associated with proliferative responses to recall Ags (memory T cells), was expressed at significantly higher levels by the PB CD4$^+$CD25$^+$ and CD4$^+$CD25$^{bright}$ populations as compared with the CD4$^+$CD25$^-$ (Fig. 2). In contrast to the PB CD4$^+$ T cells, all groups, the LP CD4$^+$CD25$^+$ and CD4$^+$CD25$^{bright}$, and CD4$^+$CD25$^-$ T cells preferentially expressed CD45RO. In contrast, the expression of CD45RA, considered a marker for naive T cells, showed the opposite expression profile. Consistent with the evidence that activated human T cells express HLA-DR molecules on their surface (54), the PB and LP CD4$^+$CD25$^+$ and CD4$^+$CD25$^{bright}$ T cells expressed significantly higher HLA-DR, as compared with the PB CD4$^+$CD25$^-$ T cells. In addition, the LP CD4$^+$CD25$^-$ T cells did express HLA-DR as compared with the PB CD4$^+$CD25$^-$ T cells (Fig. 2). Taken together, the LP CD4$^+$ T cells, regardless of CD25 expression, showed the phenotype characterized as activated memory T cells.

*LP CD4$^+$CD25$^{bright}$ T cells express CTLA-4, GITR, and Foxp3*

Since CD4$^+$CD8$^-$CD25$^+$ T cells in the PB and thymus from normal individuals are T$_R$ cells (44, 46–49), we assessed whether or



FIGURE 2. Human PB CD4$^+$CD25$^+$ (CD4$^+$CD25$^{bright}$), LP CD4$^+$CD25$^+$ (CD4$^+$CD25$^{bright}$), and CD4$^+$CD25$^-$ T cells are CD45RO$^+$, CD45RA$^-$, and HLA-DR$^+$ activated memory T cells. The cells were stained for the cell surface markers as indicated in the *upper part* of the histograms. Gates were set as described in Fig. 1. Shown is a representative experiment of a total of seven performed independently.

not the LP CD4$^+$CD25$^+$ and CD4$^+$CD25$^{bright}$ T cells also express well-known T$_R$ markers, such as CTLA-4 and GITR, although these are also known as T cell activation markers. Expectedly, both intracellular CTLA-4 and surface GITR were significantly increased in/on the LP CD4$^+$CD25$^+$ and CD4$^+$CD25$^{bright}$ T cells as compared with the LP CD4$^+$CD25$^-$ T cells (Fig. 3A). Interestingly, these markers were significantly up-regulated in/on the CD4$^+$CD25$^{bright}$ T cells as compared with the CD4$^+$CD25$^+$ T cells (Fig. 3A). However, unexpectedly, the LP CD4$^+$CD25$^-$ T cells did also express CTLA-4 intracellularly, albeit the PB CD4$^+$CD25$^-$ T cells did not (Fig. 3A). In turn, GITR on the LP CD4$^+$CD25$^-$ T cells was also up-regulated as compared with that on the PB CD4$^+$CD25$^-$ T cells (Fig. 3A). These data were also confirmed by the differences of the MFI ± SD from each population (Fig. 3A).

Recently, *Foxp3*, which encodes a forkhead/winged-helix transcription factor known as scurfin (45), was found to be expressed specifically by naturally occurring CD4$^+$CD25$^+$ T$_R$ cells, but not by previously activated CD4$^+$CD25$^+$ T cells in mice. Thus, we next questioned whether or not the LP CD4$^+$CD25$^-$ and CD4$^+$CD25$^{bright}$ T cells expressed *Foxp3*. Consistent with previous mice studies (23–25), the PB CD4$^+$CD25$^{bright}$ T population, predominantly transcribed *Foxp3*, whereas the PB CD4$^+$CD25$^-$ T cells did not (Fig. 3B). Somewhat surprising, the LP CD4$^+$CD25$^-$ T cells as well as the LP CD4$^+$CD25$^{bright}$ T cells did transcribe the gene (Fig. 3B), although the semiquantitative RT-PCR confirmed that *Foxp3* in the LP CD4$^+$CD25$^-$ T cells was clearly expressed, but to a significantly smaller extent than that in the LP CD4$^+$CD25$^{bright}$ T cells (Fig. 3C). These results indicate that T$_R$ cells may reside within the LP CD4$^+$CD25$^-$ T cell population as well as the LP CD4$^+$CD25$^{bright}$ T cell population, which expressed CTLA-4, GITR, and *Foxp3*.

*LP CD4$^+$ T cells regardless of CD25 expression are anergic*

Since the CD4$^+$CD25$^+$ T$_R$ cells show a partially anergic phenotype, we then questioned whether the LP CD4$^+$CD25$^{bright}$/CD4$^+$CD25$^-$ T cells proliferate with or without PHA, Con A, or soluble anti-CD3 mAb stimulation in the presence of MMC-treated APCs. In this proliferation assay, we first separated the CD4$^+$CD25$^{bright}$ T cells and CD4$^+$CD25$^-$ T cells from paired PBMCs and LPMCs, respectively, using a FACSVantage. In both the PB and LP CD4$^+$ T cells, the CD4$^+$CD25$^{bright}$ subsets were found to be hyporesponsive to PHA, Con A, or anti-CD3 mAb stimulation as compared with the CD4$^+$CD25$^-$ T cells (Fig. 4), indicating that the PB and the LP CD4$^+$CD25$^{bright}$ were anergic. Similarly, the PB and the LP CD4$^+$CD25$^+$ subsets were also hyporesponsive to PHA, Con A, or anti-CD3 mAb stimulation as compared with the PB and the LP CD4$^+$CD25$^-$ T cells, respectively (data not shown). Furthermore, the LP CD4$^+$CD25$^-$ T cells did proliferate to a significantly smaller extent as compared with the PB CD4$^+$CD25$^-$ T cells, indicating that the LP CD4$^+$CD25$^-$ cells were also anergic as compared with the paired PB CD4$^+$CD25$^-$ cells. However, in the presence of exogenously added rhIL-2 at the concentration of 100 U/ml, stimulation with anti-CD3 mAb elicited proliferation not only in the PB and the LP CD4$^+$CD25$^{bright}$ T cells but also in the LP CD4$^+$CD25$^-$ T cells (Fig. 4).

*LP CD4$^+$CD25$^{bright}$ T cells are regulatory*

We next investigated the regulatory properties of the LP CD4$^+$CD25$^{bright}$/CD4$^+$CD25$^-$ T cells by testing their ability to suppress the proliferative responses of the PB and LP CD4$^+$CD25$^-$ T cells obtained from the same individuals. In a series of experiments, we used the CD4$^+$CD25$^{bright}$ T cells for
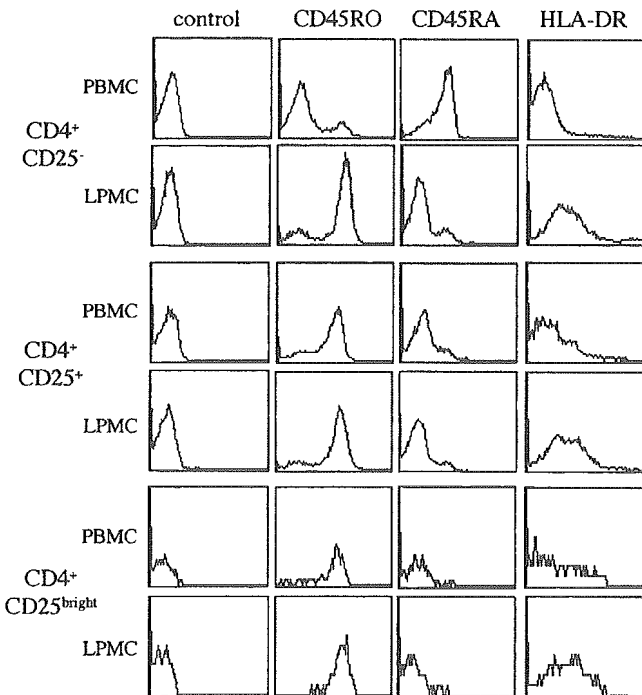
**A**



**B**

**PBMC**
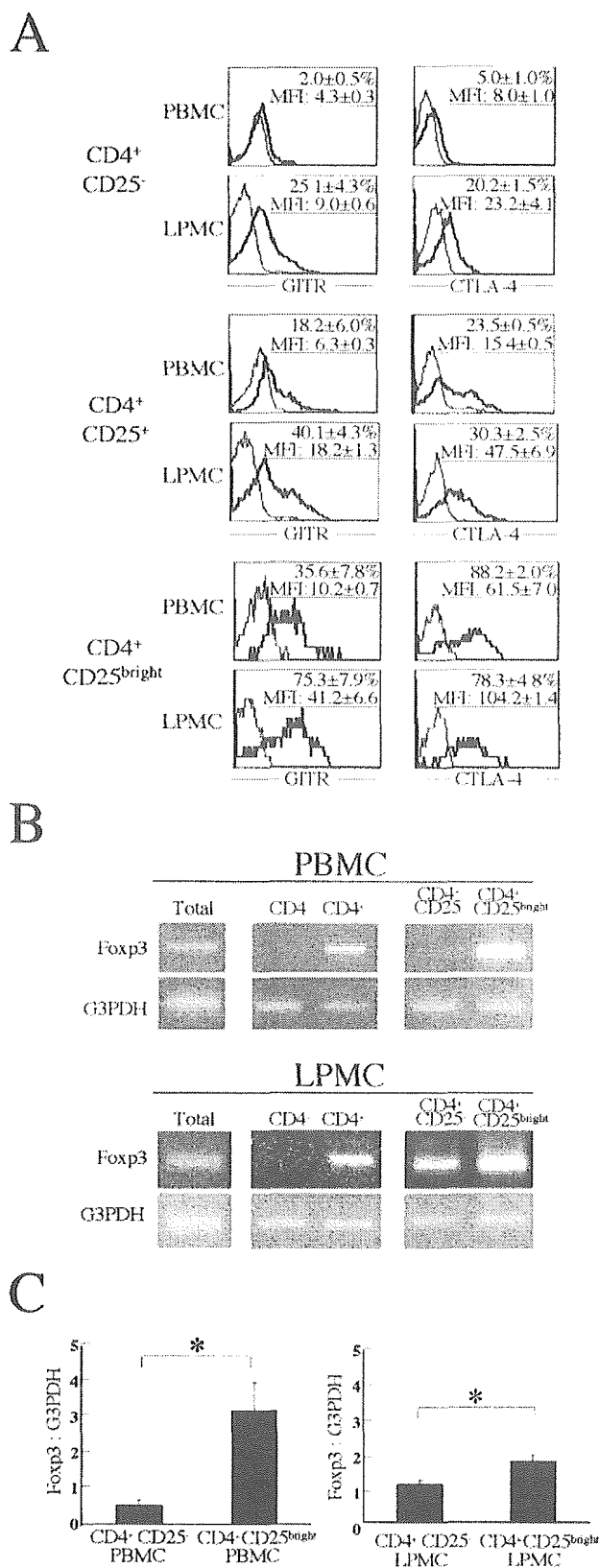


**LPMC**



**C**



**FIGURE 3.** Expression of CTLA4, GITR, and *Foxp3* in/on the PB and LP CD4⁺CD25⁻/CD4⁺CD25⁺/CD4⁺CD25$^{bright}$ T cells. *A*, The PBMCs and LP-MCs from normal individuals were collected, stained, and analyzed by flow cytometry as described in *Materials and Methods*. Histograms are gated on CD4⁺CD25⁻, CD4⁺CD25⁺, and CD4⁺CD25$^{bright}$ cells. CTLA-4 staining was performed after cell permeabilization; the isotype control is shown as a light line. The percent positive cells ± SD and the MFI ± SD from each population of four independent analyses is presented in each histogram (percent positive of GITR; PBMC, CD4⁺CD25⁻ vs CD4⁺CD25⁺, $p < 0.05$;

assessing their regulatory activity, because our preliminary data showed that the PB and LP CD4⁺CD25⁺ T cells, including CD25$^{bright}$ and CD25$^{int}$ subpopulations, did not suppress the proliferation of the PB CD4⁺CD25⁻ responder cells at a high ratio of 1 T$_R$:1 responder (data not shown). In contrast, the PB CD4⁺CD25$^{bright}$ T cells were able to suppress the proliferation of the PB CD4⁺CD25⁻ cells when cocultured at a ratio of 0.5 T$_R$:1 responder or 1 T$_R$:1 responder in the presence of MMC-treated APCs and PHA (percent proliferation compared with that at culturing with responder alone, 0.5 T$_R$:1 responder, 19.5 ± 4.4% ($p < 0.05$); 1 T$_R$:1 responder; 12.6 ± 2.6% ($p < 0.05$), $n = 7$) (Fig. 5*A*), indicating that the PB CD4⁺CD25$^{bright}$ T cells were regulatory. As a control, it was shown that titration of the same dose of the PB CD4⁺CD25⁻ cells into the cultures did not affect the degree of proliferation, thereby excluding the possibility that an increase in total responder cell number was responsible for the suppressive effect (Fig. 5*A*). However, the LP CD4⁺CD25$^{bright}$ T cells could not suppress the proliferation of the LP CD4⁺CD25⁻ responder cells even at a high ratio of 1 T$_R$:1 responder (percent proliferation, 88.5 ± 4.6% ($p = 0.32$), $n = 7$; Fig. 5*B*), probably affecting the original feature of the anergic LP CD4⁺CD25⁻ cells as shown in Fig. 4. To re-estimate their regulatory properties, we next used the PB CD4⁺CD25⁻ T cells from the same individuals as responders for the proliferation assay. Expectedly, the LP CD4⁺CD25$^{bright}$ T cells were able to suppress the proliferation of the PB CD4⁺CD25⁻ cells when cocultured at a ratio of both 0.5 T$_R$:1 responder and 1 T$_R$:1 responder (percent proliferation, 0.5 T$_R$:1 responder, 22.7 ± 4.4% ($p < 0.05$); 1 T$_R$:1 responder, 12.8 ± 2.2% ($p < 0.05$), $n = 7$; Fig. 5*C*), indicating that the LP CD4⁺CD25$^{bright}$ T cells were also regulatory. In contrast, the LP CD4⁺CD25⁻ T cells could not suppress the proliferation of the PB CD4⁺CD25⁻ cells (Fig. 5*C*), although these cells expressed CTLA-4, GITR, and *Foxp3* and were anergic (Figs. 3 and 4).

*LP CD4⁺CD25$^{bright}$ T cells suppress cytokine productions from the CD4⁺CD25⁻ T cells*

The cytokine profile of the LP CD4⁺CD25$^{bright}$ T cells and the effect of these cells on cytokines produced by the CD4⁺CD25⁻ cells were examined. After stimulation with PMA and calcium ionophore, no detectable levels of IL-2, IFN- γ, and IL-10 could be measured in both the PB and LP CD4⁺CD25$^{bright}$ T cells (Fig. 6*A*). In contrast, the PB and LP CD4⁺CD25⁻ T cells produced IL-2 and IFN-γ, but not IL-10 (Fig. 6*A*). The striking difference between the LP CD4⁺CD25$^{bright}$ and CD4⁺CD25⁻ T cell populations was that CD25$^{bright}$ cells failed to secrete IL-2, indicating

CD4⁺CD25⁻ vs CD4⁺CD25$^{bright}$, $p < 0.01$, LPMC, CD4⁺CD25⁻ vs CD4⁺CD25⁺, $p < 0.05$; CD4⁺CD25⁻ vs CD4⁺CD25$^{bright}$, $p < 0.01$; percent positive CTLA-4; PBMC, CD4⁺CD25⁻ vs CD4⁺CD25⁺, $p < 0.01$; CD4⁺CD25⁻ vs CD4⁺CD25$^{bright}$, $p < 0.005$, LPMC, CD4⁺CD25⁻ vs CD4⁺CD25⁺, $p < 0.05$; CD4⁺CD25⁻ vs CD4⁺CD25$^{bright}$, $p < 0.01$) (MFI of GITR; PBMC, CD4⁺CD25⁻ vs CD4⁺CD25⁺, $p < 0.05$; CD4⁺CD25⁻ vs CD4⁺CD25$^{bright}$, $p < 0.05$, LPMC, CD4⁺CD25⁻ vs CD4⁺CD25⁺, $p < 0.05$; CD4⁺CD25⁻ vs CD4⁺CD25$^{bright}$, $p < 0.01$; MFI of CTLA-4; PBMC, CD4⁺CD25⁻ vs CD4⁺CD25⁺, $p < 0.05$; CD4⁺CD25⁻ vs CD4⁺CD25$^{bright}$, $p < 0.005$, LPMC, CD4⁺CD25⁻ vs CD4⁺CD25⁺, $p < 0.05$; CD4⁺CD25⁻ vs CD4⁺CD25$^{bright}$, $p < 0.01$). *B*, Expression of *Foxp3* in a subpopulation of PB and LP cells. The PBMCs and LPMCs were sorted into the indicated compartments using a FACS-Vantage and nonsaturating RT-PCR analyses were conducted. *C*, Quantification of relative *Foxp3* mRNA levels in indicated CD4⁺ T cell subsets. cDNA samples were subjected to real-time semiquantitative PCR analyses, and the relative quantity of *Foxp3* in each sample was normalized to the relative quantity of G3PDH. *, $p < 0.05$.
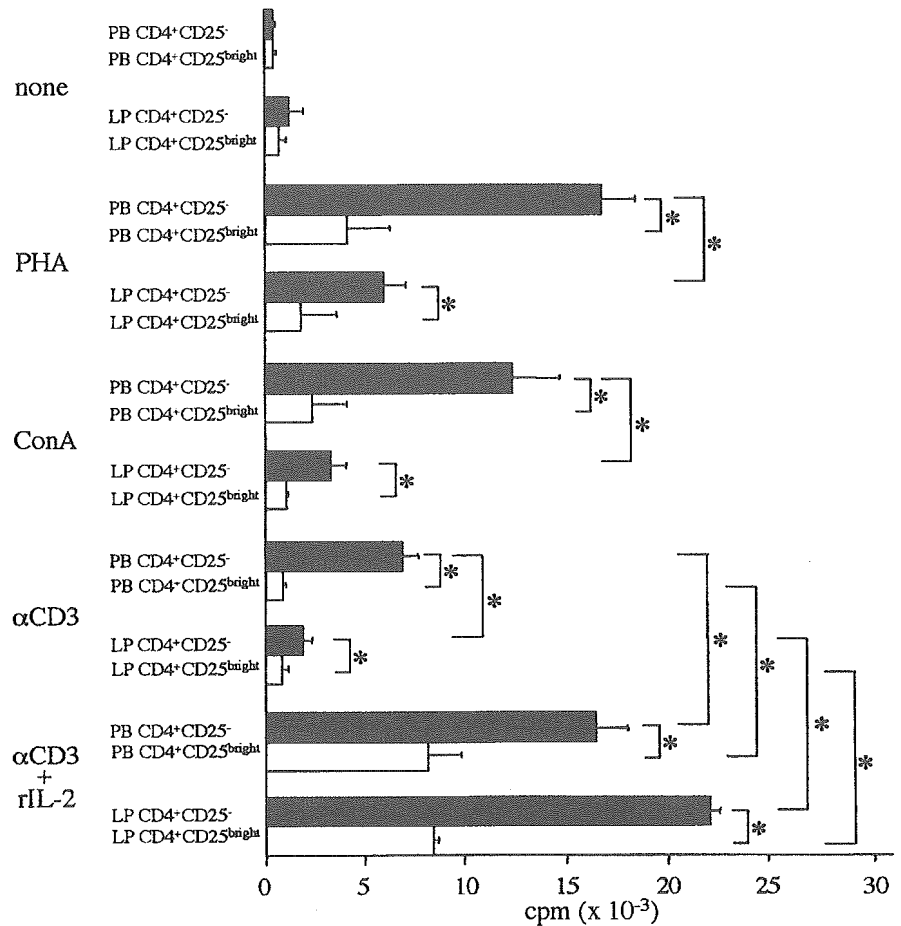
**FIGURE 4.** Proliferation of the PB and LP CD4$^+$CD25$^-$/CD4$^+$CD25$^{bright}$ T cells in response to mitogen stimulation. Cells (1 × 10$^4$) were stimulated for 72 h with or without 5 μg/ml PHA or 5 μg/ml Con A in the presence of APCs (5 × 10$^4$, MMC-treated CD4-depleted cells). *, $p < 0.05$.

that these cells have a specific defect in production of IL-2 (Fig. 6A). To next determine whether the LP CD4$^+$CD25$^{bright}$ T cells suppress cytokine secretion by CD4$^+$CD25$^-$ responder T cells, the supernatants were collected at 63 h before addition of [$^3$H]thymidine at proliferation assays and analyzed by a cytometric bead array, which allows multiparameter analysis in a single sample. As shown in Fig. 6B, although the PB CD4$^+$CD25$^-$ T cells (1 × 10$^4$ and 2 × 10$^4$ cells) in the absence of the LP CD4$^+$CD25$^{bright}$ T cells produced a large amount of IL-2, IL-5, TNF-$\alpha$, and IFN-$\gamma$, the LP CD4$^+$CD25$^{bright}$, but not the LP CD4$^+$CD25$^-$ T cells, did clearly suppress these cytokine productions, indicating that the LP CD4$^+$CD25$^{bright}$ T cell did affect not only the proliferation, but also the cytokine productions of the surrounding responder cells.

*GITR*/Foxp3 *expressions in LP T cells after TCR stimulation*

We next assessed the expression of GITR and *FoxP3* on/in LP T cells in association with activation and memory markers, because it has been reported that some anergic activated/memory T cells have regulatory properties, indicating the peripheral development of T$_R$ cells. To do so, we first divided the LP CD4$^+$ cells into CD71$^+$ (activated) and CD71$^-$ or CD45RO$^+$ (memory) and CD45RO$^-$ cells, respectively, thereafter we examined the expression of CD25/GITR and *Foxp3* using FACS and RT-PCR analysis. As shown in Fig. 7, A and B, both CD25/GITR and *Foxp3* were preferentially expressed on/in LP CD71$^+$ and CD45RO$^+$ T cells as compared with LP CD71$^-$ and CD45RO$^-$ T cells, respectively. Furthermore, the semiquantitative RT-PCR confirmed that the *Foxp3* expression in the LP CD71$^+$ and CD45RO$^+$ cells was significantly higher than that in the LP CD71$^-$ and CD45RO$^-$ cells, respectively (Fig. 7C).

Since stimulation of peripheral CD4$^+$CD25$^-$ T cells through TCR and CD28 leads to several outcomes, including the proliferation and induction of CD25 expression, it is possible that some or all of the LP CD4$^+$CD25$^{bright}$ T$_R$ cells are the result of recent activation in the periphery. As shown in Fig. 7D, both CD25 and GITR were up-regulated after the stimulation by anti-CD3/CD28 mAbs, although their expression was relatively low when compared with that of CD4$^+$CD25$^{bright}$ cells. To next determine the nature of the *Foxp3* expression in previous activation of LP T cells, we demonstrated *Foxp3* expression in both sorted CD4$^+$CD25$^-$ and CD4$^+$CD25$^{bright}$ cells stimulated with anti-CD3/CD28 mAbs. As shown in Fig. 7, E and F, anti-CD3/CD28-stimulated LP CD4$^+$CD25$^-$ cells expressed the *Foxp3* transcripts to an extent similar to that in anti-CD3/CD28-stimulated LP CD4$^+$CD25$^{bright}$ cells. However, the expression of *Foxp3* tended to be increased after the stimulation as compared with that in the starting freshly isolated population of CD4$^+$CD25$^-$ T cells, but was not significant.

*Origin of LP CD4$^+$CD25$^{bright}$ T cells*

Although human naturally arising CD4$^+$CD25$^+$ T$_R$ cells are thought to be mainly derived from thymus (46), a recent study by Walker et al. (55) suggests that *Foxp3*$^+$CD4$^+$CD25$^+$ T$_R$ can be also developed from peripheral *Foxp3*$^-$CD4$^+$CD25$^-$ T cells by in vitro anti-CD3/CD28 mAb stimulation. Furthermore, it is well known that anergic human CD4$^+$ T cells that are accompanied by an increased level of CD25 expression possess T$_R$ activity (52). Thus, it was important to determine whether our human LP CD4$^+$CD25$^{bright}$ cells were naturally arising T$_R$ cells from the thymus or anergic cells that were developed in the periphery. As one of the differences between naturally arising CD4$^+$CD25$^+$ T$_R$
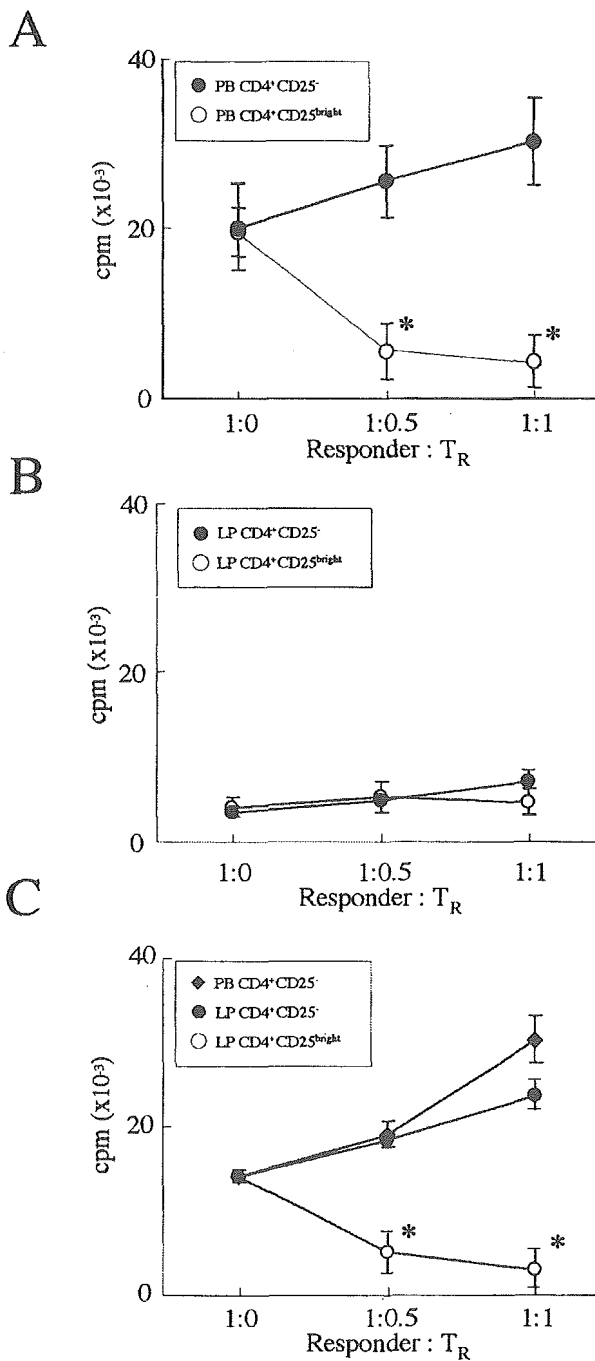
A



B



C



A



B



**FIGURE 5.** The LP CD4$^+$CD25$^{bright}$ but not the CD4$^+$CD25$^-$ T cells suppress the proliferation of the PB CD4$^+$CD25$^-$ T cells in vitro. Different doses of CD4$^+$CD25$^{bright}$ or control CD4$^+$CD25$^-$ T cells (0, 0.5 × 10$^4$, 1 × 10$^4$) were added into wells containing 1 × 10$^4$ responder PB or LP CD4$^+$CD25$^-$ cells and were stimulated with 5 $\mu$g/ml PHA in the presence of 5 × 10$^4$ MMC-treated APCs. At 63 h of culture, supernatants were taken for cytokine analysis and the cells were pulsed with 1 $\mu$Ci [$^3$H]thymidine for another 9 h. Shown is a representative experiment of seven total performed. *A*, Responders are PB CD4$^+$CD25$^-$; regulatory cells are PB CD4$^+$CD25$^{bright}$ or PB CD4$^+$CD25$^-$ (as a control). *B*, Responders are LP CD4$^+$CD25$^-$; regulatory cells are LP CD4$^+$CD25$^{bright}$ or LP CD4$^+$CD25$^-$ (as a control). *C*, Responders are PB CD4$^+$CD25$^-$; regulatory cells are LP CD4$^+$CD25$^-$, or LP CD4$^+$CD25$^{bright}$, or PB CD4$^+$CD25$^-$ (as a control). *, $p < 0.05$.

cells and anergic cells, it is well known that in vitro suppressive activity of naturally arising PB CD4$^+$CD25$^+$ T$_R$ cells usually can occur even if the T$_R$:responder ratio is >0.1 T$_R$:1 responder (49), whereas that of anergic cells can occur only if the ratio is >1 T$_R$:1
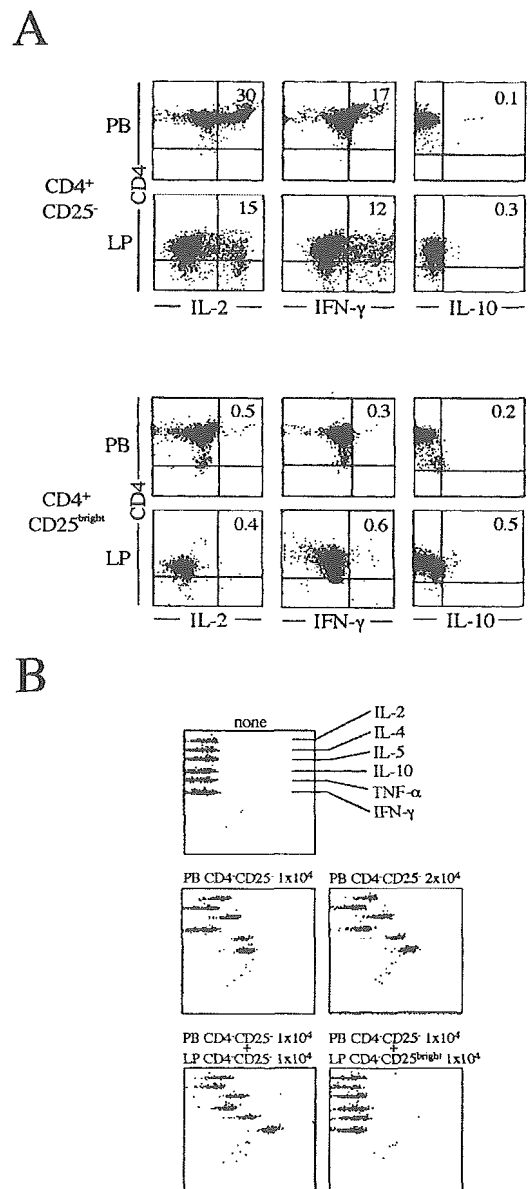
**FIGURE 6.** The CD4$^+$CD25$^{bright}$ do not secrete cytokines but can suppress the production of IL-2, IL-5, TNF-$\alpha$, and IFN-$\gamma$ by cocultured CD4$^+$CD25$^-$ cells. *A*, The frequencies of cytokine-producing cells were analyzed by gating on the CD4$^+$ subpopulation. Representatives of three independent experiments using paired PB- and LP-sorted CD4$^+$CD25$^-$/CD4$^+$CD25$^{bright}$ cells. *B*, Culture supernatants were collected from the proliferation cultures (culture supernatants from 1 × 10$^4$ or 2 × 10$^4$ PB CD4$^+$CD25$^-$ cells, 1 × 10$^4$ PB CD4$^+$CD25$^-$ plus 1 × 10$^4$ LP CD4$^+$CD25$^{bright}$ cells, and 1 × 10$^4$ PB CD4$^+$CD25$^-$ plus 1 × 10$^4$ LP CD4$^+$CD25$^-$ cells depicted in Fig. 5 before the addition of [$^3$H]thymidine incorporation. Levels of IL-2, IL-4, IL-5, IL-10, TNF-$\alpha$, and IFN-$\gamma$ were determined from culture supernatants by a cytometric bead array. Results were similar in four independent experiments.

responder (52). Furthermore, since it has been known that both the natural-occurring T$_R$ and the anergic cells require stimulation through the TCR to activate its T$_R$ program, we used soluble anti-CD3 mAb in place of PHA in this setting. Although the PB CD4$^+$CD25$^{bright}$ T cells were able to significantly suppress the proliferation of the PB CD4$^+$CD25$^-$ cells when cocultured even at a low ratio of 0.06 T$_R$:1 responder (Fig. 8*A*), the LP CD4$^+$CD25$^{bright}$ T cells could suppress only at a relatively higher ratio of >0.25 T$_R$:1 responder (Fig. 8*A*). We next conducted an

**FIGURE 7.** Expression of GITR/ *Foxp3* on/in LP T cells. *A*, Expression of CD25 and GITR on CD45RO$^+$ CD45RO$^-$ or CD71$^+$CD71$^-$ cells. Freshly isolated LPMCs from normal individuals were stained with CyChrome-anti-CD4, FITC-anti-CD25 or FITC-anti-GITR, and PE-anti-CD45RO or PE-anti-CD71 mAbs and the expression of CD25/GITR on the indicated cells was analyzed. Results were similar in four independent experiments. *B*, Expression of *Foxp3* in CD45RO$^+$CD45RO$^-$ or CD71$^+$CD71$^-$ cells. After staining with various mAbs, the indicated cells were sorted by a FACSVantage, thereafter RT-PCR analyses of *Foxp3* were conducted. Results were similar in four independent experiments. *C*, Quantification of relative *Foxp3* mRNA levels in indicated CD4$^+$ T cell subsets ($n = 5$). cDNA samples were subjected to real-time semiquantitative PCR analyses, and the relative quantity of *Foxp3* in each sample was normalized to the relative quantity of G3PDH. *, $p < 0.05$. *D*, Expression of CD25 and GITR on freshly isolated and anti-CD3/anti-CD28-stimulated LP CD4$^+$CD25$^-$ and CD4$^+$CD25$^{bright}$ cells. Freshly isolated and anti-CD3/anti-CD28-stimulated LP CD4$^+$CD25$^-$ and CD4$^+$CD25$^{bright}$ cells were stained with FITC-anti-CD25 or FITC-anti-GITR on the indicated cells. Results were similar in four independent experiments. *E*, Expression of *Foxp3* in freshly isolated and anti-CD3/anti-CD28-stimulated LP CD4$^+$CD25$^-$ and CD4$^+$CD25$^{bright}$ cells. Results were similar in three independent experiments. *F*, Quantification of relative *Foxp3* mRNA levels in indicated CD4$^+$ T cell subsets ($n = 4$). cDNA samples were subjected to real-time semiquantitative PCR analyses, and the relative quantity of *Foxp3* in each sample was normalized to the relative quantity of G3PDH. *, $p < 0.05$.
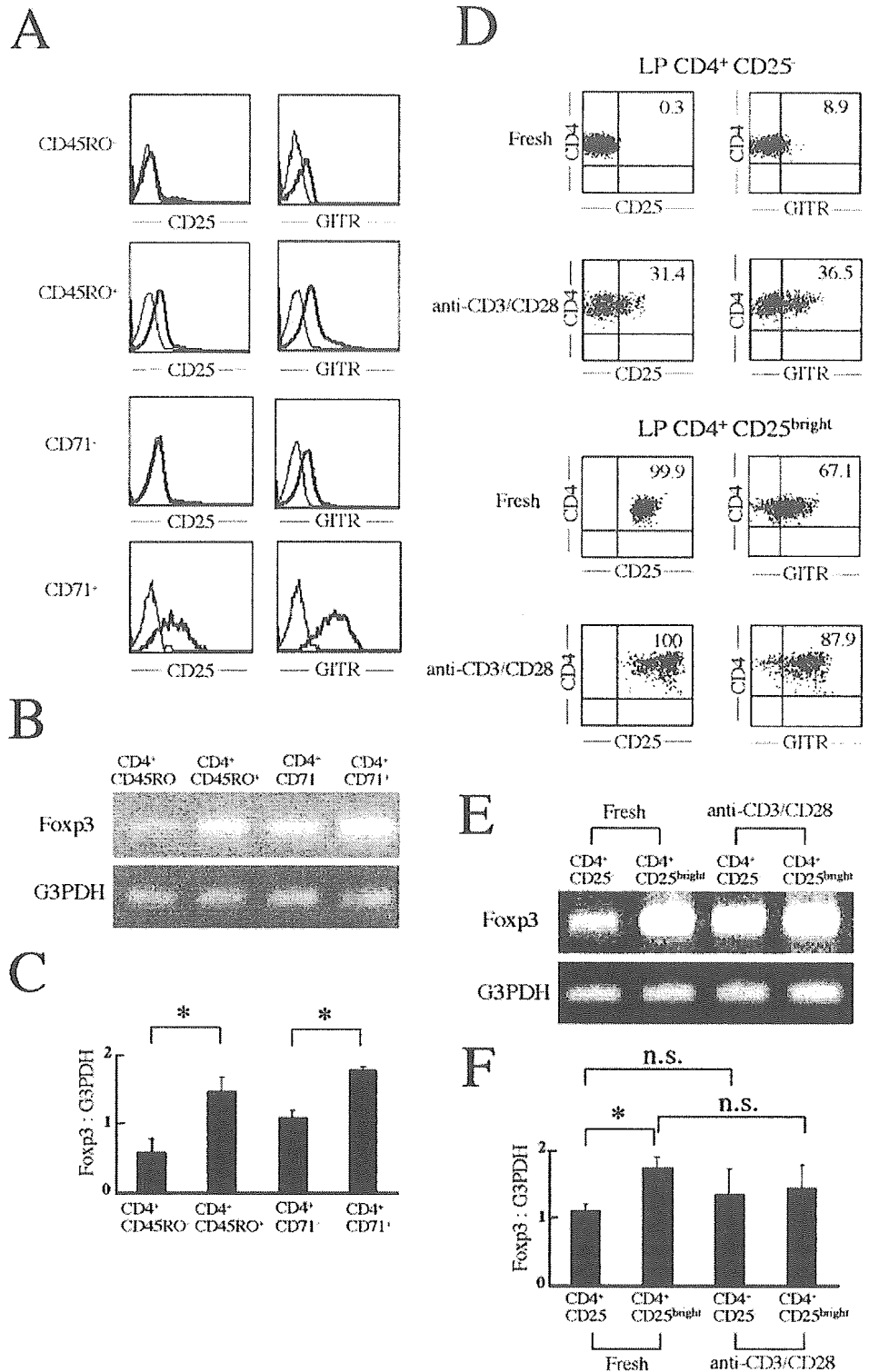


IL-2 consumption assay because it has been previously shown that low amounts of IL-2 abrogate the inhibition of the responder cells by anergic cells (52), but not by natural-occurring CD4$^+$CD25$^+$ T$_R$ cells (56). As shown in Fig. 8*B*, the LP CD4$^+$CD25$^{bright}$ cells as well as the PB CD4$^+$CD25$^{bright}$ cells could inhibit the proliferative responses of the PB CD4$^+$CD25$^-$ cells in the presence of low concentrations of IL-2 (2, 5, and 10 U/ml), but not a high concentration of IL-2 (100 U/ml), in combination with soluble anti-CD3 mAb (HIT3a, 1 μg/ml) and MMC-treated APCs. Importantly, there were no differences between the LP CD4$^+$CD25$^{bright}$

cells and the PB CD4$^+$CD25$^{bright}$ cells regarding regulatory activity at a 1:1 responder:T$_R$ ratio and at any concentrations of exogenously added IL-2.

*LP CD4$^+$CD25$^{bright}$ T cells from patients with active IBD also suppress the PB CD4$^+$CD25$^-$ T cell proliferation*

Finally, we assessed the role of CD4$^+$CD25$^+$ and CD4$^+$CD25$^{bright}$ T cells in the LP from patients with active IBD to determine whether the LP CD4$^+$CD25$^+$/CD4$^+$CD25$^{bright}$ T cells in IBD patients are activated pathogenic T cells or T$_R$ cells, which
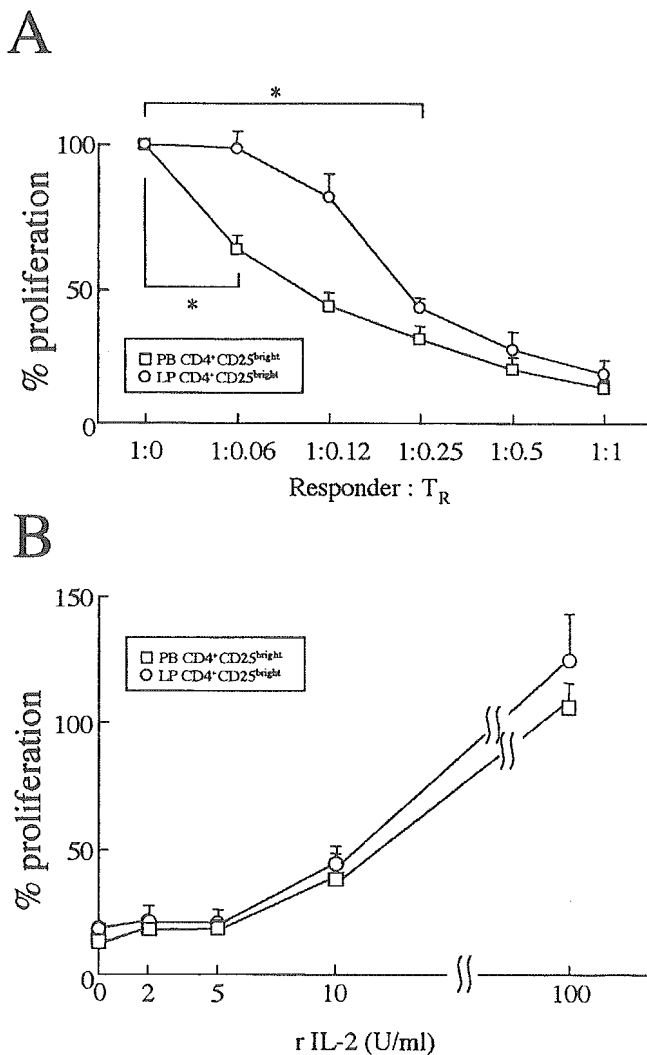
# A



# B



r IL-2 (U/ml)

**FIGURE 8.** $T_R$ activity of LP CD4$^+$CD25$^{bright}$ cells needs a higher $T_R$: responder ratio to suppress responder cells, but cannot be reversed by addition of lower concentrations of IL-2. *A*, The regulatory activities of the PB CD4$^+$CD25$^{bright}$ cells and the LP CD4$^+$CD25$^{bright}$ cells were examined. The PB CD4$^+$CD25$^-$ responder cells (1 × 10$^4$ cells/well) and various numbers of the PB CD4$^+$CD25$^{bright}$ cells or the LP CD4$^+$CD25$^{bright}$ cells (0–1 × 10$^4$ cells/well) were stimulated with soluble anti-CD3 mAb (HIT-3a, 1 $\mu$g/ml) and MMC-treated autologous APCs (5 × 10$^4$ cells/well). The mean percent inhibition of the proliferative response by CD4$^+$CD25$^{bright}$ cells was calculated. *B*, The effects of culturing the PB CD4$^+$CD25$^-$ responder cells (1 × 10$^4$ cells/well) with MMC-treated APCs (5 × 10$^4$ cells/well) and increasing concentrations of exogenous IL-2 in the presence of the same numbers of the PB CD4$^+$CD25$^{bright}$ cells or the LP CD4$^+$CD25$^{bright}$ cells (1 × 10$^4$ cells/well) is shown. Results were similar in four independent experiments. *, $p < 0.05$.

should be cells opposite of each other in terms of their pathogenesis. As shown in Fig. 9, *A* and *B*, both the LP CD4$^+$CD25$^+$ and CD4$^+$CD25$^{bright}$ T cells were significantly increased in patients with active CD or active UC as compared with normal individuals. Of note, the percentages of the LP CD4$^+$CD25$^{bright}$ T cells per total LP CD4$^+$CD25$^+$ T cells were also significantly increased in IBD patients compared with those of normal individuals (Fig. 9*C*). Although Barrat et al (57) recently reported a combination of immunosuppressive drugs, vitamin D$_3$ and dexamethasone, induced human and mouse naive CD4$^+$ T cells to differentiate in vitro into IL-10-producing regulatory T cells (named Tr1), there were no correlations between the medical treatments and the CD25

expression in IBD patients (data not shown). Similarly to the normal LP CD4$^+$ T cells, the LP CD4$^+$CD25$^-$ T cells as well as the LP CD4$^+$CD25$^+$ and CD4$^+$CD25$^{bright}$ T cells from IBD patients did express intracellular CTLA-4 and surface GITR, although their expression was apt to be less than in/on the LP CD4$^+$CD25$^{bright}$/CD4$^+$CD25$^+$ T cells (Fig. 9*D*). Furthermore, the LP CD4$^+$CD25$^{bright}$, but not CD4$^+$CD25$^-$ T cells from active IBD patients, did suppress the proliferation of the paired PB CD4$^+$ CD25$^-$ T cells to an extent similar to that of the normal LP CD4$^+$ CD25$^{bright}$ T cells (Fig. 9*E*), indicating that the LP CD4$^+$CD25$^{bright}$ T cells from IBD patients contain protective CD4$^+$CD25$^{bright}$ $T_R$ cells.

## Discussion

In the present study, we demonstrated that the LP CD4$^+$CD25$^{bright}$ T cells isolated from normal human individuals possessed regulatory activity. Of particular importance, although many mucosal immunologists believed so far that the activated LP CD25$^+$ T cells that were accumulated in the inflamed mucosa of IBD patients should be pathogenic, we also demonstrated that not only these cells and particularly their subpopulation of CD4$^+$CD25$^{bright}$ T cells from IBD patients were significantly increased as compared with those from normal individuals, but also the LP CD4$^+$CD25$^{bright}$ T cells from IBD patients retained regulatory activity to an extent similar to that of normal individuals. These results indicate that the LP CD4$^+$CD25$^{bright}$ $T_R$ cells should be involved at least in part in the local T cell homeostasis both in normal and inflammatory conditions.

Although accumulating evidence shows that human PB and thymic CD4$^+$CD8$^-$CD25$^+$ T cells possess regulatory activity (46–49) with the same characteristics in mice, Baecher-Allan et al. (44) recently demonstrated that only CD4$^+$CD25$^{bright}$, but not the whole CD4$^+$CD25$^+$ T cells, have regulatory activity. This indicates that the whole CD4$^+$CD25$^+$ T cells contain a relatively high proportion of previously activated T cells rather than naturally occurring CD4$^+$CD25$^{bright}$ $T_R$ cells, thereby the freshly isolated whole CD4$^+$CD25$^+$ T cells cannot suppress the proliferation of autologous CD4$^+$CD25$^-$ T cells in coculture. Consistent with their report, we also detected $T_R$ activity in the fraction of the PB and LP CD4$^+$CD25$^{bright}$, but not in the whole CD4$^+$CD25$^+$ T cells. Furthermore, the evidence that the LP CD4$^+$CD25$^{bright}$ T cell fraction rather than whole CD4$^+$CD25$^+$ T cells in patients with IBD was significantly increased as compared with normal individuals may indicate that the LP CD4$^+$CD25$^{bright}$ T cells function to control or down-modulate the excessive immune responses in inflamed mucosa of IBD patients. In support of this, it has recently been shown that CD4$^+$CD25$^+$ $T_R$ cells can reverse the established intestinal inflammation in CD4$^+$CD45RB$^{high}$ T cell-transferred colitic mice (58).

However, the question arises as to why the patients with active IBD in this study were obligated to receive the surgical operation because of the limitation by the conventional drug therapy to control the severe inflammation, although the increased LP CD4$^+$CD25$^{bright}$ $T_R$ cells resided in the inflamed mucosa. We believe that the answer lies in the fact that the high levels of various cytokines (e.g., IL-2, IL-6, and IL-15) that are produced in severely inflamed mucosa from active IBD patients (40) and the up-regulated expression of costimulatory molecules, such as CD80 and CD86, and class II MHC molecules (40), thereby these would abolish the regulatory activity of the LP CD4$^+$CD25$^{bright}$ $T_R$ cells and enhance the LP CD4$^+$ T cell activation in situ. In line of this hypothesis, first, two reports (59, 60) revealed that not only a high
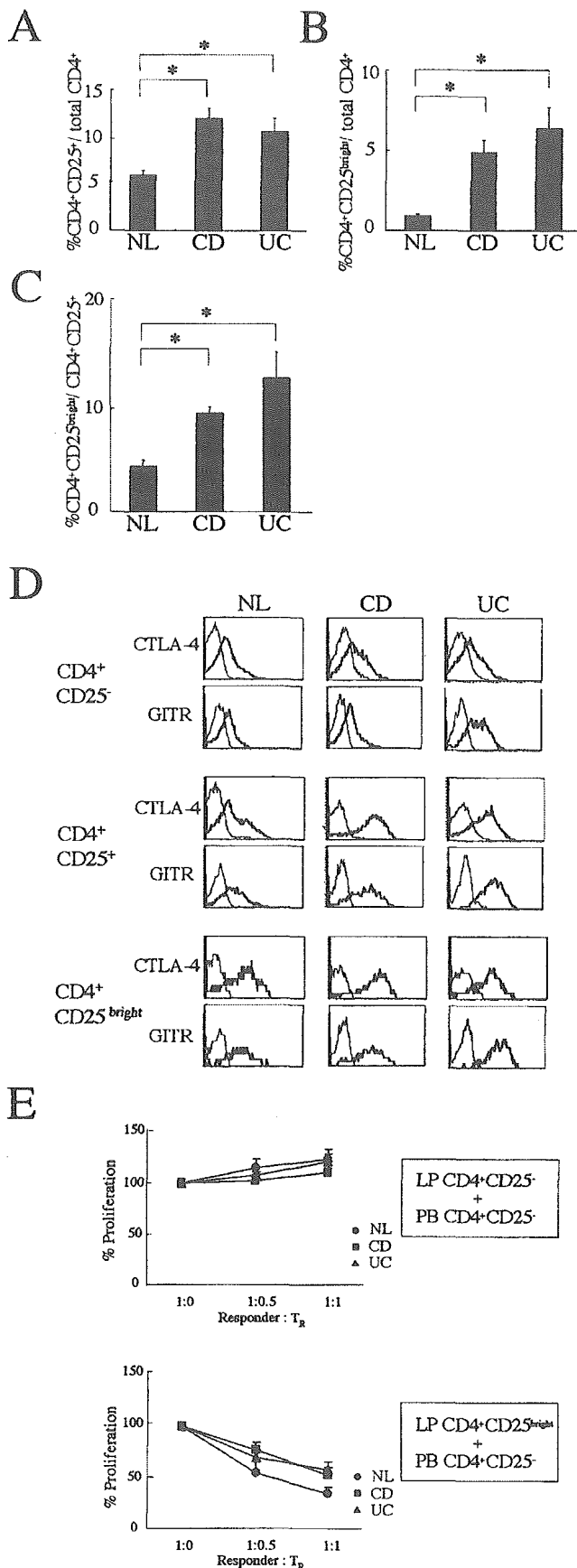
**FIGURE 9.** LP CD4$^+$CD25$^{bright}$ T cells from IBD patients also possess regulatory activity. *A*, The percentages of the LP CD4$^+$CD25$^+$ T cells in total CD4$^+$ cells isolated from normal individuals (NL, $n$ = 15), patients with UC ($n$ = 13), and patients with CD ($n$ = 17) were determined by a FACSCalibur. *, $p$ < 0.05. *B*, The percentages of the LP CD4$^+$CD25$^{bright}$

dose of IL-2 along with TCR stimulation triggers their proliferation and neutralizes the suppressive activity during their proliferation, but also upon removal of IL-2, the suppression-broken CD4$^+$CD25$^+$ T cells revert to their original suppressive state. Second, IL-6 produced by activated dendritic cells in response to TLR ligand during chronic inflammation is critical for T cell activation and efficient blockade of T$_R$ activity (61). Thus, the possibility cannot be excluded that the increased LP CD4$^+$CD25$^{bright}$ T$_R$ cells do not function well at the site of severe inflammation, thereby our patients could not overcome their intestinal inflammation by the conventional drug therapy, such as corticosteroids and immunosuppressants. We are now investigating whether additional IL-2 or IL-6 affects the suppressive activity of the LP CD4$^+$ T cells in an in vitro assay and the correlation between the number of the LP CD4$^+$CD25$^{bright}$ T$_R$ cells and clinical course, especially the onset of IBD.

Furthermore, it was very important to determine whether or not the LP CD4$^+$CD25$^{bright}$ T$_R$ cells were identical to the PB CD4$^+$CD25$^{bright}$ T$_R$ cells originally described by others (46–49) in terms of their origin. Unlike the PB CD4$^+$CD25$^{bright}$ T$_R$ cells that could suppress responder cells even at a T$_R$:responder ratio of 0.06 T$_R$:1 responder in the presence of soluble anti-CD3 mAb, the LP CD4$^+$CD25$^{bright}$ T$_R$ cells needed a relatively higher responder:T$_R$ ratio of 0.25 T$_R$:1 responder to suppress the responders in the same setting. Like the PB CD4$^+$CD25$^{bright}$ T$_R$ cells, however, the suppression by the LP CD4$^+$CD25$^{bright}$ T$_R$ cells could not be reversed by addition of lower amounts of IL-2 (2–10 U/ml). Although it might well be that in this special situation, mucosal T$_R$ activity is relatively mild as compared with the PB CD4$^+$CD25$^{bright}$ T$_R$ cells, it is likely that the LP CD4$^+$CD25$^{bright}$ T$_R$ cells are derived mainly from natural-occurring T$_R$ cells because the suppression by the LP T$_R$ cells was observed at <1 T$_R$:1 responder (0.5 T$_R$:1 responder and 0.25 T$_R$:1 responder) and was not caused by IL-2 consumption in our analysis.

Besides the natural-occurring CD4$^+$CD25$^{bright}$ T$_R$ cells and the anergic cells, the existence of other distinct groups of T$_R$ cells, such as Tr1 cells and Th3 cells and their role in controlling intestinal inflammation along with suppressor cytokines IL-10 and TGF-$\beta$, should also be considered (4). As a possibility, two groups have recently reported data suggesting that contact with CD4$^+$CD25$^+$ T$_R$ cells causes CD25$^-$ responder T cells to become suppressive themselves, the mechanism of which is referred to as "infectious tolerance," although its cytokine dependency is still controversial (37, 62). This mechanism of infectious tolerance could explain not only how such a small LP CD4$^+$CD25$^{bright}$ population (1–2%) of cells can regulate a much larger population of responder cells in vivo, but also how the LP CD4$^+$CD25$^-$ and CD4$^+$CD25$^{int}$ T cells could express CTLA-4, GITR, and *Foxp3*.

The functions of mucosal T cells are largely uncertain, but cells with a "memory" phenotype predominate in both the epithelium and the LP, indicating that they have been exposed to Ags (40). Thus, LP CD4$^+$ T cells may be of particular importance to local